

Black Hole Horizons as Patternless Binary Messages and Markers of Dimensionality

Szymon Łukaszyk*

Łukaszyk Patent Attorneys, ul. Głowackiego 8, 40-052 Katowice, Poland

This study aims to reconcile quantum theory with the universality of the speed of light in vacuum and its implications on relativity, through an information-theoretic approach. We introduce the concepts of a holographic sphere and variational potential. Entropy variation expressed in terms of information capacity of this sphere results in the concept of binary potential in units of negative, squared speed of light in vacuum. Accordingly, the event horizon is a fundamental holographic sphere in thermodynamic equilibrium with only one exterior side: a noncompressible binary message that maximizes Shannon entropy. Therefore, the Jordan–Brouwer separation theorem and generalized Stokes theorem do not hold for black holes. We introduce the concept of inertial potential and demonstrate its equivalence to the variational potential, which ensures that any inertial acceleration represents a nonequilibrium thermodynamic condition. We introduce the concept of the complementary time period and relate it with the classical time period through integral powers of the imaginary unit to formulate the notions of unobservable velocity and acceleration, which are perpendicular and tangential to the holographic sphere, respectively, and bounded with the observable velocity and acceleration based on Pythagorean relations. We further discuss certain dynamics scenarios between the two masses. The concept of black hole informationless emission is introduced as a complement to informationless Bekenstein absorption and extended to arbitrary wavelengths. Black hole quantum statistics with degeneracy interpreted as the number of Planck areas on the event horizon are discussed. The study concludes that holographic screens and equipotential surfaces are spherical equivalents, and every observer is a sphere in nonequilibrium thermodynamic condition. Lastly, we propose a solution to the black hole information paradox.

Keywords: entropic gravity; black hole information paradox; Shannon entropy; Landauer’s principle; Axis of Evil (cosmology); black hole quantum statistics; exotic \mathbb{R}^4 ; imaginary time; no-hiding theorem

1. Introduction

An uncharged, nonrotating (Schwarzschild) black hole (BH) can be observed as a 2-sphere; however, one cannot state anything regarding its interior [1], which is equivalent to the fact that it does not have any interior. However, mathematical 2-spheres possess an interior. In general, any $(n - 1)$ -dimensional topological sphere in \mathbb{R}^n forms a common boundary of two connected components: bounded interior and unbounded exterior, as asserted by the Jordan–Brouwer separation theorem. However, this theorem does not hold for BHs thereby disapproving the correctness of our intuitive concept of the physical space represented as \mathbb{R}^3 (or \mathbb{R}^4). Additionally, the generalized Stokes theorem does not hold for BHs. A differential form over a BH event horizon does not equal the integral of its exterior derivative over the BH interior, considering there is no such thing as a BH interior which is a (-1) -dimensional void (the empty set) with zero volume and an undefined surface.

A BH elevates John Archibald Wheeler’s “*it from bit*” conclusion, which states that there is no such thing as space or time or spacetime continuum [2] beyond the microscopic level. This causes us to research nature as a vertex-labeled graph (graph of nature) with certain intrinsic properties reflecting the 2nd law of thermodynamics. The primordial Big Bang singularity (the first point or vertex) expanded this graph of nature into dimensionalities and not into a four-dimensional spacetime [3].

The combinatorial proof of the *H*-theorem derived by Ludwig Boltzmann in 1877 [4] introduced energy quanti-

zation, which resulted in the development of quantum theory [5] and created the measurement problem that demands an interpretation. To date, no consensus has been achieved in the scientific community regarding the universal validity of any particular interpretation of the measurement problem [6].

The author is convicted that life is an explanation of the measurement problem performed *hic et nunc* by any particular observer. The measurement yields rational (as rational numbers) and classical (as bits, not qubits) information that is twofold, considering it relates both to the *without* [exterior] and *within* [interior] of things. Quoting Pierre Teilhard de Chardin, “In the eyes of the physicist, nothing exists legitimately, at least up to now, except the *without* of things. The same intellectual attitude is still permissible in the bacteriologist, whose cultures (apart from some substantial difficulties) are treated as laboratory reagents. But it is already more difficult in the realm of plants. It tends to become a gamble in the case of a biologist studying the behavior of insects or coelenterates. It seems merely futile with regard to the vertebrates. Finally, it breaks down completely with man, in whom the existence of a *within* can no longer be evaded, because it is the object of a direct intuition and the substance of all knowledge” [7].

Albert Einstein believed [8] that “the experience of the *now* means something special for man, something essentially different from the past and the future, but that this important difference does not and cannot occur within physics. That this experience cannot be grasped by science seemed to him a matter of painful but inevitable resignation. (...) there is something essential about the *now* which is just outside of the realm of science.” The

* szymon@patent.pl

author strongly disagrees with this statement: the 3-dimensional universe emerges out of an uncountably infinite-dimensional graph of nature during observer-dependent measurement. The observer-independent measurements simply do not exist [9, 10, 11]. A local time associated with each observer in special relativity is reversible. Nonetheless, we can now investigate time in other conceptual contexts [12], especially as an emergent, entropic quantity².

Presumably, dimension n is a complex number, wherein biological evolution is possible only in dimension $n = 3 + i$ with 3 spatial dimensions and imaginary time owing to the exotic \mathbb{R}^4 property of such space [3], which dimensionality was exploited by biological evolution from among uncountably infinite other dimensionalities. Particularly, the only real imaginary number is $0i = 0$. This zero is the *nunc*, that is the moment that passes for every living biological cell, and it cannot be placed outside the realm of science [8, 12]. Therefore, Lorentz transformations denote the rotations of a 4-ball of a fixed radius R , expressed as

$$x^2 + y^2 + z^2 + (ict)^2 = R^2. \quad (1)$$

Rather than aiming to propose new physics, this research aims to seek a new meaning to the existing, experimentally verified physical theories, especially to the theory of relativity, as it is grounded on the objective, unobservable, extra-instantaneous existence of 3D physical reality (*the universe*), and hence, is not complete.

This paper is structured as follows. Sections 2 and 3 present the discretization in terms of the Planck units and the discrete BHs, respectively. Section 4 introduces the concept of a BH informationless emission as complementary to informationless Bekenstein absorption and extend it to arbitrary wavelengths. Subsequently, the author's perspective on the entropic gravity derivation disclosed in [14] along with a simplified model of the spherical universe with two masses is presented in Section 5. Thereafter, the concept of the variational potential and the entropy variation sphere is proposed in Section 6 to display the equivalence of known entropic gravity equations. Section 7 presents the concept of the binary potential to exemplify that an event horizon is a binary message that maximizes the Shannon entropy. The concept of inertial potential is introduced in Section 8. The concept of complementary time period related with *classical* time period by integral powers of imaginary unit is introduced in Section 9, which includes the kinematics of the two masses on a holographic sphere are, and the significant radii of a constant mass. Section 10 summarizes the Bose–Einstein, Maxwell–Boltzmann, and Fermi–Dirac statistics with degeneracy interpreted as the number of Planck areas on a BH event horizon. Lastly a solution to BH information paradox is proposed in Section 11.

The author is of the opinion that the notion of charge and other already unified quantities should emerge from

² “Einstein imagined himself riding a photon. But (...) we are too heavy to ride photons or electrons. We cannot possibly replace such airy beings, identify ourselves with them, and describe what they would think, if they were able to think, and what they would experience, if they were able to feel anything” ([12] p. 219).

topological and entropic considerations, and hence, charged BHs were deliberately neglected from the considerations of this study.

Baroque derivations were used to support certain controversial claims that largely deviate from the mainstream understanding of physics.

Natural units were also deliberately neglected from the considerations of this study to avoid loss of clarity. The meaning of all seven constants of nature used in this study: c (speed of light in vacuum), e (the base of the natural logarithm), G (the gravitational constant), h (the Planck constant), i (the imaginary unit), k_B (the Boltzmann constant), and π (the ratio of a circle's circumference to its diameter), should not be treated without careful considerations.

A two-dimensional Boolean lattice (a holographic screen), evolving with time, deduced from unitarity, entropy, and counting arguments has been proposed in [13] to explain the failure of developing completely consistent mathematical models of quantum BHs. This research aims to pursue this idea further in an attempt to reconcile quantum theory with the universality of the speed of light in vacuum and its implications on relativity, in an information-theoretic approach.

2. Discretizations

Discretization in terms of Planck units was adopted in certain segments of this study. These “natural units of measure” introduced by Max Planck in 1899 “are independent of special bodies or substances, thereby necessarily retaining their meaning for all times and for all civilizations, including extraterrestrial and non-human ones” [15].

Where deemed appropriate, uppercase letters denote dimensional quantities and lowercase letters denote the Planck units or their multipliers. Masses M were considered as real multiplicities m of the Planck mass m_p without loss of generality (w.l.o.g.), expressed as

$$M \doteq mm_p \quad m \in \mathbb{R}. \quad (2)$$

Additionally lengths were considered w.l.o.g. as the real multiplicities of the Planck length ℓ_p . Particularly, sphericity was considered w.l.o.g. in terms of the diameter d or radius r multipliers

$$D \doteq d\ell_p \quad R \doteq r\ell_p \quad d, r \in \mathbb{R}. \quad (3)$$

However, the wavelengths were considered as

$$\lambda \doteq l\ell_p \quad l \in \mathbb{R} \setminus \{(-1, 1)\}, \quad (4)$$

considering the wavelength denotes the distance over which the shape of the wave repeats, and this distance must be at least equal to the Planck length. No physical models describe smaller lengths, and hence the open set $(-1, 1)$ is forbidden.

Based on Eqs. (2) and (4), the relation between wavelength l and mass multiplier m can be derived in terms of the Compton wavelength, expressed as

$$\lambda_M \doteq l\ell_p = \frac{h}{cm m_p} \Leftrightarrow lm = 2\pi. \quad (5)$$

On constraining to $l \geq 1$, we get

$$m \leq 2\pi, \quad (6)$$

which can be called the *threshold of distinguishability*, considering it indicates that the Compton wavelengths of masses $M \geq 2\pi m_P$ (1.37E-7 kg) are smaller than the Planck length, which is physically impossible. Such masses no longer exhibit the wave-particle duality and would not interfere with each other in the double-slit experiment. In principle, they are neither bosonic nor fermionic (nor anyonic) and are distinguishable at all instances. Evidently, this does not preclude the distinguishability of lighter masses.

The possible meaning of real and/or negative masses, wavelengths, and diameters is discussed in Sections 4, 8, 10, and in the Appendices of this paper. The complex wavelength multipliers l expressed in Eq. (4) are briefly discussed in Sections 4 and 10. Overall, detailed investigations of these notions are beyond the scope of this study.

3. Discrete Black Holes

On expressing the mass and diameter of the BH w.l.o.g. using Eqs. (2) and (3), respectively, the Schwarzschild diameter can be expressed as

$$D_{BH} = \frac{4Gm_{BH}}{c^2} \sqrt{\frac{\hbar c}{G}} = 4m_{BH} \ell_P, \quad (7)$$

yielding a simple relationship between the BH mass and the diameter or radius multipliers, given as

$$m_{BH} = \frac{d_{BH}}{4} = \frac{r_{BH}}{2}. \quad (8)$$

Therefore, the BH Compton wavelength (5) can be expressed as

$$l_{BH} = \frac{2\pi}{m_{BH}} = \frac{8\pi}{d_{BH}} \left(\lambda_{BH} = \frac{2\ell_P^2}{R_{BH}} = \frac{4\ell_P^2}{D_{BH}} \right), \quad (9)$$

and constraining to $l \geq 1$, the BH *threshold of distinguishability* (6) can be rewritten in terms of a BH diameter or radius multipliers as

$$d_{BH} \leq 8\pi, \quad \text{or} \quad r_{BH} \leq 4\pi. \quad (10)$$

Therefore, only the BHs with diameter (radius) multipliers below this threshold are adequately small to have Compton wavelengths (5) greater than the Planck length. As we shall see in Section 4, BH threshold of distinguishability (10) is equal to a threshold of BH collapsibility (22).

Eq. (3) was used to determine the information capacity of an event horizon as $N_{BH} = \pi D_{BH}^2 / \ell_P^2 = \pi d_{BH}^2$. Moreover, the BH surface gravity (82) was combined into the Hawking radiation formula to derive the Hawking radiation temperature T_{BH} as a function of N_{BH} or diameter multiplier d_{BH}

$$T_{BH} = \frac{1}{2\pi d_{BH}} T_P, \quad (11)$$

as shown in Fig. 1, where T_P denotes the Planck temperature (cf. Appendix 1).

Given that no physical models define temperatures greater than the Planck temperature, the primordial Big Bang singularity temperature corresponds to a BH with $d_{BH} = 1/(2\pi)$, $N_{BH} = 1/(4\pi)$, and $[N_{BH}] = 0$. This is in accordance with the Heisenberg's uncertainty principle for a single degree of freedom (67). Furthermore, the natural diameter multiplier d_{BH} can be related to the 2π -cycle: BH temperature (11) decreases by a factor of 2π with every integer increment of d . At $d_{BH} = 1$, BH is at a temperature $T_{BH} = T_P/2\pi$, which is a reduced Planck temperature, similar to the reduced Planck constant or reduced wavelength. The BH Hagedorn temperature of approximately 1.7E12 K — *the boiling point of ordinary matter* — is achieved by using the BH with $d_{BH} \approx 1.33\text{E}19$, equivalent to $D_{BH} = 2.14\text{E}-16$ m, which is approximately $1/4$ of a proton charge radius (8.41E-16 m).

Table 1 summarizes certain examples of discrete BHs and displays the information capacity, number of bits, mass, and temperature of each hole as a function of its diameter multiplier d_{BH} .

Table 1: Examples of discrete BHs

$d_{BH} = D_{BH}/\ell_P$	$N_{BH} = \pi d_{BH}^2$	$[N_{BH}]$	$M_{BH}/m_P = d_{BH}/4$	$T_{BH}/T_P = 1/(2\pi d_{BH})$	BH type/comments
$1/(2\pi)$	0.0796	0	0.0398	1	The Big Bang (Planck temperature)
$1/\pi$	0.3183	0	0.0796	0.5	Half of Planck temperature
$1/\sqrt{\pi}$	1	1	0.1410	0.2821	min 1-bit, MB stat. 1 st singularity
$\sqrt{\ln(4)/\pi}$	$2\ln(2)$	1	0.1661	0.2396	Landauer 1 st bound ($M_{BH}c^2 = T_{BH}k_B \ln(2)$)
$\sqrt{2/\pi}$	2	2	0.1995	0.1995	min 2-bit, FD stat. 1 st singularity
$2\sqrt{\ln(2)/\pi}$	$4\ln(2)$	2	0.2349	0.1694	Landauer 2 nd bound (BH entropy)
1	π	3	0.25	0.1592	π -bit, surface gravity equals Planck acc.
$\sqrt{4/\pi}$	4	4	0.2821	0.1410	min 4-bit, one unit of entropy
$\sqrt{2}$	2π	6	0.3536	0.1125	imaginary Planck time at the BH hrz.
2	4π	12	0.5	0.0796	12-bit, HUP yields $R_{BH} = \ell_P$
4	16π	50	1	0.0398	$M_{BH} = m_P$
2π	$4\pi^2$	124	1.5708	0.0253	Margolus-Levitin theorem threshold
$4\sqrt{\pi}$	$16\pi^2$	157	1.7725	0.0224	Threshold of informationless stability
8π	$64\pi^2$	1984	2π	$1/(16\pi^2)$	$M_{BH} = 2\pi m_P$, thr. of distinguishability
1.58E45	7.88E90	7.88E90	3.9606E44	1.0071E-46	Sagittarius A*

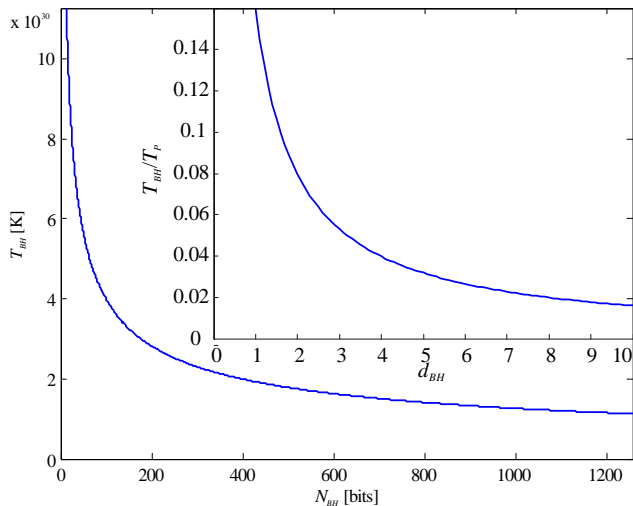


Fig. 1: Black hole temperature T_{BH} as a function of its information capacity N_{BH} and diameter multiplier d_{BH} .

Any vertex v on the surface of an n -ball is related with a certain vertex p , which is the center of this n -ball by the same parameter called radius R . Formally, for a set of vertices V with a generalized distance function $\mu \geq 0$ (cf. Appendix 5), the surface of the n -ball is defined as

$$B(p) = \{v \in V \mid \mu(v, p) = R\}. \quad (12)$$

However, this definition does not hold for BHs in any dimension n . As BHs do not have interiors (the empty set is a BH interior), no vertex p of the graph of nature can be the BH center. Therefore, to define a BH as a centerless $(n-1)$ -sphere, the pairs of vertices on its surface must be related to each other through the same diameter D_{BH} . Therefore, the event horizon of a BH can be defined as

$$B_{BH}(p \in \emptyset) = \left\{ \begin{array}{l} \forall v_i \in V \exists! v_j \in V \cap \forall v_k \in V \exists! v_l \in V \\ \mu(v_i, v_j) = \mu(v_k, v_l) = D_{BH} \cap \\ \mu(v_i, v_k) = \mu(v_j, v_l) \end{array} \right\}. \quad (13)$$

Each vertex of the event horizon is associated with precisely one vertex based on the relationship of the diameter D_{BH} , and each pair of vertices non-associated to the relationship of the diameter D_{BH} is associated with each other based on the distance relationship equal to the that of their D_{BH} partners. This definition requires at least four vertices defining two diameters, as shown in Fig. 2(b) (the lines in the figure do not indicate line segments passing across a BH interior). Therefore, the term Schwarzschild radius is a misnomer.

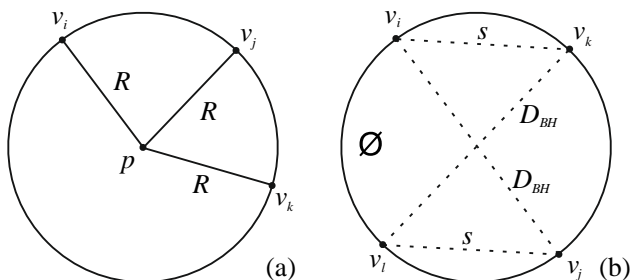


Fig. 2: Surface of (a) n -ball, (b) BH.

However, the definition (13) is inappropriate for small BHs. Two micro-BHs in \mathbb{R}^3 with triangulated event horizons are shown in Fig. 3, wherein π -bit BH ($R_{BH} = \ell_p/2$)

comprises four vertices and 4π -bit BH ($R_{BH} = \ell_p$) comprises eleven vertices with the fractional part (52) containing six triangles around the equator. As shown, only the latter event horizon defines only one, precise diameter relation between its two poles 1 and 11. Notably, neither a 1-bit nor a 2-bit BH allows the triangulation.

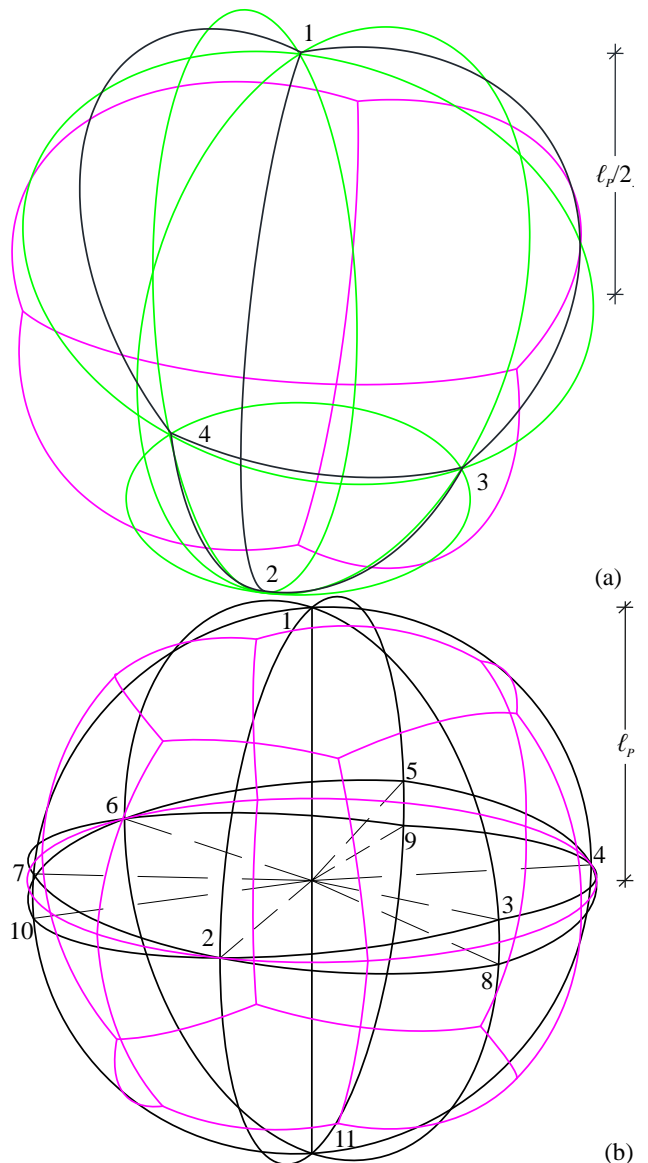


Fig. 3: Axonometric views of micro-BHs with Voronoi tessellation (pink). (a) Unipolar π -bit BH and. (b) Bipolar 4π -bit BH.

The Euclidean space \mathbb{R}^n , researched as a simplicial n -manifold (i.e., triangulated for $n=2$), inherits a natural topology from \mathbb{R}^n . Moreover, such an approach disentangles the topological (metric-independent) and geometric (metric-dependent) content of the modelled quantities [16, 17]. Therefore, Planck areas on holographic spheres and BHs horizons must be triangular.

BHs are by no means stable entities, as discussed in the subsequent section.

4. Black Hole Diameter Fluctuations

BH energy increases if a photon of energy $E = hc/\lambda = Mc^2$ is incident on a BH event horizon. If we intend to lose all photon information, it should have a sufficiently long wavelength to ensure that the point of collision with the horizon is uncertain [18, 19 (p. 160)]. Therefore, its wavelength must be greater than or equal to

the BH radius (26). This thought experiment was famously devised by Jacob Bekenstein to derive a threshold for BH entropy (44). If we assume the condition of equality ($\lambda = R_{BH}$), the Compton mass of the photon is $M = h/(cR_{BH})$, and hence, the new BH radius would be

$$R_{BH}^A = R_{BH} + \delta R = \frac{2GM_{BH}}{c^2} + \frac{2G}{c^2} \frac{h}{cR_{BH}}, \quad (14)$$

the new BH area would be

$$A_{BH}^A = A_{BH} + \delta A = 4\pi(R_{BH} + \delta R)^2, \quad (15)$$

and the new BH information capacity would be

$$N_{BH}^A = 64\pi^3 \frac{\ell_p^2}{R_{BH}^2} + 32\pi^2 + 4\pi \frac{R_{BH}^2}{\ell_p^2}. \quad (16)$$

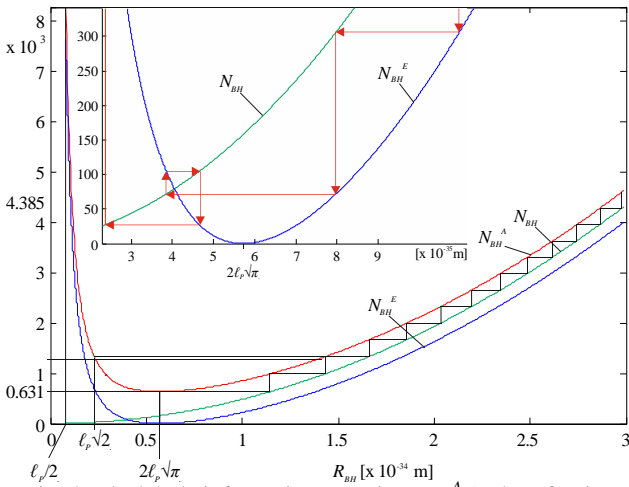


Fig. 4: Black hole information capacity: N_{BH}^A (red) - after informationless absorption, N_{BH}^E (blue) - after informationless emission, N_{BH} (green) - initial information capacity.

Eq. (16) attains the minimum for $R_{BH} = 2\ell_p\sqrt{\pi}$, as shown in Fig. 4. The BH with this radius (and mass equal to $m_p\sqrt{\pi}$) will increase its information capacity fourfold from $N_{BH} = (4\pi)^2$ to $N_{BH}^A = (8\pi)^2$ after absorbing the photon with mass $M = m_p\sqrt{\pi}$. Furthermore, a transmission of another photon with a wavelength corresponding to the new BH radius will increase its information capacity. For radii distinct from $2\ell_p\sqrt{\pi}$, the same BH information capacity can be obtained for two distinct initial radii, and consequently, for two distinguished photon energies.

The informationless BH absorption, depicted by Eq. (16), can be reversed to produce the informationless BH emission: we do not intend to know the point of emission on the event horizon. Therefore, by reversing the steps Eqs. (14)–(16) and subtracting δR , we get

$$N_{BH}^E = 64\pi^3 \frac{\ell_p^2}{R_{BH}^2} - 32\pi^2 + 4\pi \frac{R_{BH}^2}{\ell_p^2}, \quad (17)$$

which defines the BH information capacity after emitting a photon with wavelength corresponding to its radius. The emission was explained by Hawking [20] and contributes to collapsibility of micro-BHs.

The emission N_{BH}^E (17) fluctuates around $R_{BH} = 2\ell_p\sqrt{\pi}$, shown in the inset of Fig. 4, and increases for $R_{BH} < 2\ell_p\sqrt{\pi}$, despite the emission of the wavelength.

These fluctuations should be considered along with the absorption (16). Upon considering both the processes together, the BH mass along with its diameter fluctuates with time.

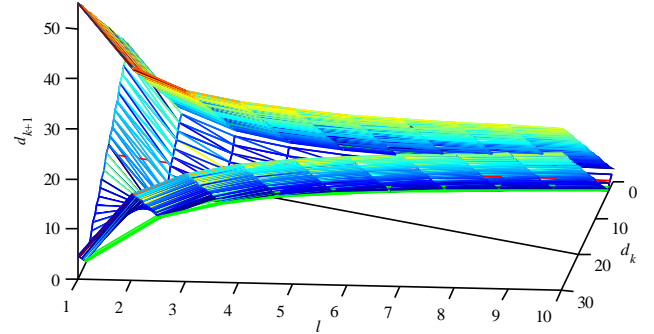


Fig. 5: New 2-sphere BH diameter d_{k+1} having initial diameter d_k after absorption or emission of a wavelength l . Sinusoidal characteristic of collapse is due to l drawn as a natural number.

For the informationless case, shown in Fig. 4, $d = 2l$.

The informationless absorption (16) and emission (17) can be extended (cf. Appendix 3) to arbitrary wavelengths l (in general, shedding the informationless property) as

$$N_{BH}^{A/E}(d, l) = 64\pi^3 \frac{1}{l^2} \pm 16\pi^2 \frac{d}{l} + \pi d^2, \quad (18)$$

which can be described more compactly ($N_{BH} = \pi d_{BH}^2$) as a recurrence relation

$$d_{k+1}^{A/E} = \sqrt{64\pi^2 \frac{1}{l^2} \pm 16\pi \frac{d_k}{l} + d_k^2}, \quad (19)$$

where d_{k+1} is a new diameter of the BH (2-sphere) with an initial diameter d_k after absorption (A, “+”) or emission (E, “-”) of a mass with the Compton wavelength l , as shown in Fig. 5.

This derivation can be extended to other dimensions n , thereby yielding the following recurrence relation for a BH, $(n - 1)$ -sphere, diameter after absorption (A, “+”) or emission (E, “-”) of a wavelength l

$$\left(d_{k+1}^{A/E}\right)^{n-1} = \left(d_k \pm \frac{8\pi}{l}\right)^{n-1}. \quad (20)$$

The RHS of Eq. (20) shows an initial state, whereas the LHS shows the final state of a BH after absorption/emission of a wavelength l .

Table 2: Black hole information capacity N_{BH} in integer dimensions $n = -7, -5, \dots, 9$.

n	$N_{BH}(n)$	n	$N_{BH}(n)$
-7	$3360/(\pi^4 d^8)$	3	πd^2
-5	$-240/(\pi^3 d^6)$	4	$\pi^2 d^3/4$
-3	$24/(\pi^2 d^4)$	5	$\pi^3 d^4/6$
-1	$-4/(\pi d^2)$	6	$\pi^3 d^5/32$
0	0	7	$\pi^3 d^6/60$
1	2	8	$\pi^4 d^7/384$
2	πl	9	$\pi^4 d^8/840$

Following the limits of one-sided thermodynamic equilibrium, the BHs can certainly be studied in $(n + i)$ -dimensions with $n \neq 3$, which renders them as markers of dimensionality. Table 2 summarizes the information ca-

capacities as the functions of the diameter multiplier d for BHs in a range of integer dimensions [21].

Particularly, if n is odd, then

$$N_{BH}(n)N_{BH}(2-n) = 4(-1)^{\lfloor n/2 \rfloor}. \quad (21)$$

There are at least three distinct thresholds of a BH collapse after the emission of wavelength l , which can be postulated in Eq. (20):

1. $d_{k+1}^E = 0$ total collapse;
2. $d_{k+1}^E = 1/(2\pi)$ Planck temperature collapse; and
3. $d_{k+1}^E = 1/\sqrt{\pi}$ one-bit collapse.

The total BH collapse occurs after the emission of wavelength $l = 8\pi/d_k$, i.e., after the emission of its entire Compton mass (9). For Sagittarius A*, $l \leq 1.59e-44 \ll 1$, so Sagittarius A* will never collapse.

Table 3: Emission wavelength l maintaining constant BH diameter as in integer dimensions $n+i = -7, -6, \dots, 9$.

$n+i$	Emitted l maintaining constant BH diameter
-7, 9	$l_1 = \frac{4\pi}{d_k}, l_{2,3,4,5} = \frac{4\pi}{d_k} \left(1 \pm i\sqrt{3 \pm 2\sqrt{2}} \right)$ $l_{6,7} = \frac{4\pi}{d_k} (1 \pm i)$
-6, 8	complicated and complex solution
-5, 7	$l_1 = \frac{4\pi}{d_k}, l_{2,3} = \frac{4\pi}{d_k} (1 \pm \sqrt{3}i), l_{4,5} = \frac{4\pi}{d_k} \left(1 \pm \frac{\sqrt{3}}{3}i \right)$
-4, 6	$l_{1,2,3,4} = \frac{4\pi}{d_k} \left(1 \pm \frac{\sqrt{5 \pm 2\sqrt{5}}}{\sqrt{5}}i \right)$
-3, 5	$l_1 = \frac{4\pi}{d_k}, l_{2,3} = \frac{4\pi}{d_k} (1 \pm i)$
-2, 4	$l_{1,2} = \frac{4\pi}{d_k} \left(1 \pm \frac{\sqrt{3}}{3}i \right)$
-1, 3	$l = 4\pi d_k$
0, 2	contradiction ($1 \neq 0$)
1	identity ($1 = 1$)

If we set $l \geq 1$ in (20), we obtain

$$d_k = 8\pi \approx 25.132, \quad (22)$$

for $d_{k+1}^E = 0$,

$$d_k = 8\pi + \frac{1}{2\pi} \approx 25.292, \quad (23)$$

for $d_{k+1}^E = 1/2\pi$, and

$$d_k = 8\pi + \frac{1}{\sqrt{\pi}} \approx 25.697, \quad (24)$$

for $d_{k+1}^E = 1/\sqrt{\pi}$, which are the thresholds for the maximum diameter multipliers of collapsible BHs. The lowest threshold $d_k = 8\pi$ corresponds to a BH with mass 2π times greater than the Planck mass. This threshold has been already derived as Eq. (10) by considering the BH Compton wavelength and shall be further delivered in Eq. (89)

by considering the variational potential (78) on the event horizon (88).

The BH diameter does not vary ($d_{k+1}^E = d_k$) after the emission of wavelengths listed in Table 3. Eq. (20) is symmetrical w.r.t. $n = 1$, i.e., the wavelengths solving $d_{k+1}^E = d_k$ are the same for n and $2 - n$, which is a reflection relation around 2. According to prior research [22], an ordinary space of $(m - 2)$ -dimension is equivalent to the m -dimensional superspace with an anticommuting coordinate, and a 4 space with only one anticommuting coordinate (time) is equivalent to an ordinary space with negative dimensions of -2 .

The analytical formula $l(m)$ for constant diameter emission in any dimension, if one exists, remains to be researched. The odd dimensionalities admit the real wavelength $l = 4\pi/d_k$ corresponding to precisely half the BH Compton wavelength (9). In even dimensionalities, all constant diameter wavelengths l are complex, thereby indicating the existence of a link with vanishing real volumes and surfaces of m -balls, in even, negative dimensions (owing to the vanishing rational factor g_m , not because of the vanishing diameter) [21].

5. Entropic Work of Gravity

Entropic gravity defines that both inertia and gravity are phenomena emergent on a holographic screen, whereas the classical concepts such as position, velocity, acceleration, mass, and force³ are far from obvious [23]. Quoting Erik Verlinde, “when a particle has an entropic reason $[\delta S]$ to be on one side [displaced by δR] of the membrane [holographic screen] and the membrane carries a temperature $[T]$, it [the particle] will experience an effective force $[F]$ equal to $[\delta W =] F\delta R = T\delta S$ ” [23, Eq. 3.3].

Based on this entropic work formula, the Second law of Newton [23, Eq. 3.5] can be recovered by combining the Unruh temperature T [23, Eq. 3.4] with the postulated variation of entropy δS near the screen [23, Eq. 3.2], linearized with respect to the reduced Compton wavelength $\lambda = \hbar/Mc$ by introducing inertial mass M to this equation. Newton’s law of gravity [23, Eq. 3.9] can be recovered by assuming a sphere partitioned into Planck areas ℓ_P^2 . Instead of the Unruh effect, temperature is derived from the equipartition theorem [23, Eq. 3.7] for a degree of freedom, multiplied by the number of these areas. Particularly, the mass–energy equivalence $E = M_2c^2$ [23, Eq. 3.8] introduces the 2nd gravitational mass M_2 to the equation. Entropic, emergent gravity [23] has been experimentally confirmed to date [24].

The same entropic work equation can be derived [14] using an entropy formula [14, Eq. 1] that reduces to the Bekenstein–Hawking entropy at the event horizon. As such, the temperature [14, Eq. 2] is obtained using the Hawking formula and expressed as the gradient of the gravitational potential of the 2nd gravitational mass M_2 , which further reduces to the BH temperature at the event horizon. This derivation is certainly compelling to those agreeing with Verlinde’s perspective concerning the entropic origin of gravity and inertia, and provides new insights into this matter. Let us delve more closely at this derivation.

³ Time is not included in this enumeration [23, p. 2].

As shown in Fig. 6, we considered a model of a closed 3-dimensional spherical, universe \mathbb{R}^3 with an edge of $\partial\mathbb{R}^3$. The concept of an edge $\partial\mathbb{R}^3$ is certainly a strong abuse of notation and does not indicate that the Euclidean space \mathbb{R}^3 is *closed*. However, this concept can be introduced in (36), for instance, to prove that the surface integral vanishes if the edge $\partial\mathbb{R}^3$ is moved to infinity. Regardless, we cannot consider Euclidean space \mathbb{R}^3 without a universe to investigate it in. Based on our current knowledge, the radius of the observable universe is approximately 46 billion light years.

At its center, our toy universe contains a Schwarzschild BH with (passive) mass M_{BH} . Its presence is much more formally inconveniencing than the that of the edge $\partial\mathbb{R}^3$, considering it does not contain an interior.

Passive mass M_{BH} generates a conservative and irrotational gravitational field that can be expressed in terms of a scalar, gravitational potential ϕ_g as

$$\phi_g = -\frac{GM_{BH}}{R}, \quad (25)$$

for $R \geq R_{BH}$, where

$$R_{BH} = \frac{2GM_{BH}}{c^2} \quad (26)$$

represents the radius of the BH event horizon.

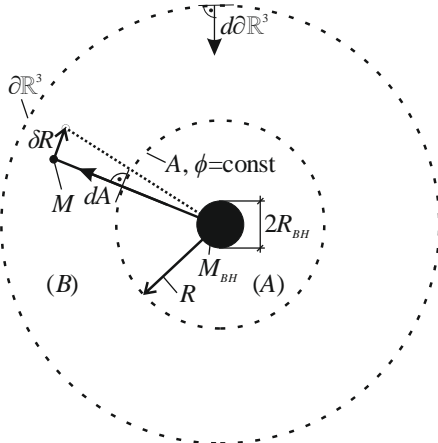


Fig. 6: Simplified model of universe used in this study.

The minimum potential ϕ_g occurs at the event horizon and amounts to

$$\phi_{BH} = -\frac{GM_{BH}}{R_{BH}} = -GM_{BH} \frac{c^2}{2GM_{BH}} = -\frac{1}{2}c^2. \quad (27)$$

An equipotential surface A surrounds the M_{BH} in a volume (A) for $R \geq R_{BH}$. Thus, the single-mass M_{BH} system is described by Laplace's equation:

$$\nabla^2 \phi_g = 0. \quad (28)$$

Let us now consider a test mass M located in the background of M_{BH} in volume (B) , such that $(A) + (B) = \mathbb{R}^3$ and $B = A \cup \partial\mathbb{R}^3$. Owing to this simplified model of a spherical universe including two masses, we do not encounter the three-body problem, and yet this model can adequately demonstrate all the current findings of this study. Moreover, owing to its spherical symmetry, R is the only significant dimension. The system of these

two masses M_{BH} and M can be described using Poisson's equation for gravity, given as

$$\nabla^2 \phi_g = 4\pi G\rho, \quad (29)$$

where ρ is the mass density in the volume (B) comprising M . Poisson's Eq. (29) is the inhomogeneous version of Laplace's Eq. (28) and includes the latter, if $\rho = 0$. This is satisfied on any equipotential surface A , and integrating over (A) using the divergence theorem yields

$$4\pi G \iiint_{(A)} \rho dV_A = \iiint_{(A)} \nabla^2 \phi_g dV_A = \oint\oint_A \nabla_R \phi_g dA, \quad (30)$$

where ∇_R is the potential gradient (25), which is the derivative in the direction of the normal vector on the surface A pointing outside the volume (A) .

Newton's law of gravity (48) is a general physical law derived from empirical observations. In this case, the passive mass M_{BH} is located at the center of the simplified model of the spherical universe, which implies that the spherically symmetric gravitational potential $\phi_g(R)$ (25) and mass density $\rho(R)$ satisfy Laplace's equation (28). The 2nd mass M and all the subsequent test masses introduced to this model would induce mass density inhomogeneity and attain the same equilibrium in a *free fall* process induced by $\nabla_R \phi_g$, unless work is done to disturb it.

Such a disturbing force F — applied to wiggle the test mass M location by a certain δR in a time period δt (doing work δW) — equals to the corresponding variation of the potential energy in volume (B) , expressed as

$$\begin{aligned} \delta W = F \circ \delta R = \delta U &= -\iiint_{(B)} \phi_g \delta \rho dV_B = \\ &= -\frac{1}{4\pi G} \iiint_{(B)} \phi_g \nabla^2 \delta \phi dV_B, \end{aligned} \quad (31)$$

where Eq. (29) is used to express the variation in density $\delta \rho$ in the volume (B) containing, the now active, mass M with the corresponding variation $\delta \phi$ of the potential. Let us refer to δR as the disturbing radius of the active mass M .

Accordingly, integrating Eq. (31) over $(B) = \mathbb{R}^3 - (A)$, we get

$$-4\pi G \delta U = \iiint_{\mathbb{R}^3} \phi_g \nabla^2 \delta \phi dV - \iiint_{(A)} \phi_g \nabla^2 \delta \phi dV_A, \quad (32)$$

and introducing the 2nd and 3rd terms that negate each other, we get

$$\begin{aligned} -4\pi G \delta U &= \iiint_{\mathbb{R}^3} \phi_g \nabla^2 \delta \phi dV - \iiint_{(A)} \delta \phi \nabla^2 \phi_g dV_A + \\ &+ \iiint_{(A)} \delta \phi \nabla^2 \phi_g dV_A - \iiint_{(A)} \phi_g \nabla^2 \delta \phi dV_A \end{aligned}, \quad (33)$$

Thereafter, the Green's second identity was used to transform the 3rd and 4th terms to surface integrals, as

$$\begin{aligned} -4\pi G \delta U &= \iiint_{\mathbb{R}^3} \phi_g \nabla^2 \delta \phi dV - \iiint_{(A)} \delta \phi \nabla^2 \phi_g dV_A + \\ &+ \oint\oint_A (\delta \phi \nabla_R \phi_g - \phi_g \nabla_R \delta \phi) dA \end{aligned}. \quad (34)$$

Moreover, the 4th term was integrated over the equipotential surface A to displace the potential ϕ_g before the integral, and the divergence theorem (30) was applied to retrace to the volume integration over (A) . However the 4th term vanished upon employing Poisson's equation (29), considering $\delta\phi$ contained no sources inside (A) . Subsequently, the 2nd term with the volume integration over (A) was further re-expressed as an integration over $(A) = \mathbb{R}^3 - (B)$

$$-4\pi G\delta U = \iiint_{\mathbb{R}^3} \phi_g \nabla^2 \delta\phi dV - \iiint_{\mathbb{R}^3} \delta\phi \nabla^2 \phi_g dV + \iiint_{(B)} \delta\phi \nabla^2 \phi_g dV_B + \oiint_A \delta\phi \nabla_R \phi_g dA \quad (35)$$

Similarly, the 3rd term vanished considering ϕ_g included no sources inside (B) . Therefore, using Green's second identity to transform the volume integral over \mathbb{R}^3 into the surface integral over $\partial\mathbb{R}^3$, we get

$$-4\pi G\delta U = \oiint_{\partial\mathbb{R}^3} (\phi_g \nabla_R \delta\phi - \delta\phi \nabla_R \phi_g) d\partial\mathbb{R}^3 + \oiint_A \delta\phi \nabla_R \phi_g dA \quad (36)$$

where the 1st surface integral over $\partial\mathbb{R}^3$ vanished as well. Therefore,

$$F \circ \delta R = \delta U = -\frac{1}{4\pi G} \oiint_A \nabla_R \phi_g \delta\phi dA. \quad (37)$$

This innovative procedure conveniently transformed the volume integration Eq. (31) over (B) defining the universe \mathbb{R}^3 with a hole (A) into a surface integration Eq. (37) over the equipotential surface A describing only this hole, which expresses the BH M_{BH} event horizon for a limiting case of $R = R_{BH}$.

Both the uniform inertial, that is flat space-time acceleration (a) and the gravitational acceleration (g) can be related to temperature T according to Unruh blackbody-radiation equation

$$T_a = \frac{\hbar}{2\pi c k_B} a, \quad (38)$$

or the analogous Hawking blackbody-radiation equation

$$T_g = \frac{\hbar}{2\pi c k_B} g. \quad (39)$$

Thus, the temperature can be expressed in terms of the gravitational potential gradient (25) as

$$T_g = \frac{\hbar}{2\pi c k_B} \nabla_R \phi_g. \quad (40)$$

To eventually derive the Verlinde's entropic gravity, the variation of entropy on A [14, Eq. (1)⁴] should be expressed using another function

$$\delta S = -\frac{c k_B}{2G\hbar} \delta\phi A, \quad (41)$$

which expresses the entropy variation as a function of the variation of the potential $\delta\phi$ induced upon relocating the active mass M in volume (B) by δR , which corresponds to the variation in density $\delta\rho$ in the volume (B) , according to Eq. (31)

$$\delta dS = -\frac{c k_B}{2G\hbar} \delta\phi dA \quad (42)$$

on surface element dA of the surface A .

Thereafter, $\nabla_R \phi_g$ from Eq. (40) and $\delta\phi$ from Eq. (42) were substituted into Eq. (37), which demonstrates that this is equal to the entropic work

$$F \circ \delta R = -\frac{1}{4\pi G} \oiint_A \left(\frac{2\pi c k_B}{\hbar} T_g \right) \left(-\frac{2G\hbar}{c k_B} \delta dS \right) = \oiint_A T_g \delta dS = T_g \oiint_A \delta dS = T_g \cdot \delta S \quad (43)$$

where T_g can be displaced before the integral, due to integrating over an equipotential surface A . Therefore, work δW and force F can be deemed entropic. The author conjectures that all forces are entropic. Thus, work is both the scalar product of force and variation of location and the regular product of temperature and variation of entropy. However, this does not preclude the additional variations of force and temperature.

As discussed in Section 7, the concept of binary potential Eq. (54) transforms the entropy variation Eq. (41) on the equipotential surface A into a distribution of bits Eq. (55) on the holographic screen A , thereby rendering the latter as more general than Eq. (41). The author of [14] reported that the "number N of 'bits' on the screen made no appearance here" (i.e., in the derivation of Eq. (43)), and apparently disregarded the vitality of a "bit" in relation to the BH information paradox. The entropy formula (41) certainly does not relate well to electrodynamic [14], as it reduces to BH entropy [18] (using (27)) as

$$S_{BH} = -\frac{c k_B}{2G\hbar} \phi_{BH} A_{BH} = \frac{k_B c}{2G\hbar} \frac{c^2}{2} A_{BH} = \frac{1}{4} k_B N_{BH}. \quad (44)$$

which is a thermodynamical term. Notably, the entropy of any BH is equal to that of the Schwarzschild hole with the same area (by Penrose process).

Eq. (44) can be extended to Eq. (41) beyond the event horizon for an arbitrary equipotential A and $\delta\phi$. However, for radii smaller than the Schwarzschild radius (26), it is meaningless, and hence disproves assumption **B** of [14] that \mathbb{R}^3 is made up by the union of nonintersecting holographic screens. Screens *passing across* BHs cannot be defined, and therefore, they create voids in such a *holographized* \mathbb{R}^3 . Thus, if we relied only on the intuitive concept of *space*, we could use neither the divergence theorem nor the Green's second identity in the derivation Eq. (43). However, they are valid, and we have used them correctly. Our intuition was misleading.

Neither Verlinde's (46) nor Hossenfelder's (41) entropy equations should be considered as an entropic explanation of any physically observed inverse-square law. Both

⁴ The additive constant in this equation can represent the fractional part $\{N_A\}$ of an equipotential surface information capacity.

these equations are related, which will be discussed in the subsequent section.

6. Entropy Variation Sphere and Variational Potential

We compare Hossenfelder’s entropy variation equation (41) with Verlinde’s formula for the variation in entropy in vicinity of a holographic screen, expressed as [23, Eq. 3.1]

$$\delta S = 2\pi k_B \quad \text{when} \quad \delta R = \frac{\hbar}{Mc}, \quad (45)$$

or [23, Eq. 3.2]

$$\delta S = 2\pi k_B \frac{Mc}{\hbar} \delta R = 2\pi k_B \frac{\delta R}{\lambda_M}, \quad (46)$$

in the case a test mass M approaching the screen. 2π was included in δS , considering it is apparently related to the *threshold of distinguishability* (6).

Eq. (46) enables the recovery of the second law of Newton, considering a from the Unruh temperature (38) to define

$$\begin{aligned} F \circ \delta R = T_a \cdot \delta S &= \frac{\hbar}{2\pi c k_B} a \cdot 2\pi k_B \frac{Mc}{\hbar} \delta R = \\ &= Ma \cdot \delta R \Leftrightarrow F = Ma = M \frac{\delta R}{\delta t^2} \end{aligned}, \quad (47)$$

and Newton’s law of gravity, considering Hawking temperature (40) in terms of the gravitational potential (25) of the passive mass M_{BH} to derive

$$\begin{aligned} F \circ \delta R = T_g \cdot \delta S &= \frac{\hbar}{2\pi c k_B} \left(\frac{GM_{BH}}{R^2} \right) \cdot 2\pi k_B \frac{Mc}{\hbar} \delta R = \\ &= \frac{GM_{BH}M}{R^2} \cdot \delta R \Leftrightarrow F = \frac{GM_{BH}M}{R^2} \end{aligned}. \quad (48)$$

Alternatively, the original Verlinde’s procedure can be used with the Hawking temperature (40) induced by the equipartition theorem for a single degree of freedom and mass–energy equivalence, as described in the beginning of this Section. Furthermore, Verlinde’s Eq. (46) directly introduces the Unruh temperature T_a (38) as

$$\begin{aligned} Ma \circ \delta R = T_a \cdot \delta S &= T_a \cdot 2\pi k_B \frac{Mc}{\hbar} \delta R \Leftrightarrow \\ a &= \frac{2\pi c k_B}{\hbar} T_a \end{aligned}. \quad (49)$$

However, none of these laws can be recovered from Eq. (41), whose starting point is the gravitational potential (25) analyzed in the context of Poisson’s equation for gravity (29). Therefore, the current approach investigated the recovery of these laws.

Let us define the potential variation on the equipotential surface A , induced by wiggling the active mass M location by δR , as gravitational potential (25) (with “–“)

$$\delta\varphi \doteq -\frac{GM}{\delta R} = -\frac{G}{\delta R} \frac{\hbar}{c\lambda_M}. \quad (50)$$

This ensures that the equipotential surface A is a sphere of the disturbing radius δR . We shall further refer to this potential as the “variational potential” and the corresponding sphere as the “entropy variation sphere.” By substituting Eq. (50) into Eq. (41), we recovered Verlinde’s entropic equation (46) as

$$\delta S = -\frac{ck_B}{2G\hbar} \left(-\frac{GM}{\delta R} \right) 4\pi\delta R^2 = 2\pi k_B \frac{Mc}{\hbar} \delta R, \quad (51)$$

and hence, we recovered Newton’s also the second law and law of universal gravitation.

As expressed in Eq. (50), the hypothesis concerning the variational potential $\delta\varphi$ is a consequence of the entropic work derivation presented in [14]. At the onset, A is assumed to surround BH M_{BH} in \mathbb{R}^3 , as shown in Fig. 6, and is not related to δR . However, after completing the derivation, A solely represents a 2-sphere, a set of points situated at a fixed distance from a BH event horizon; each distance pointing into some virtual central point located within the BH with no interior. Eq. (41) describes the potential variation on the equipotential surface, whereas Eq. (46) was motivated by Bekenstein’s original thought experiment [18], which resulted in the BH entropy formula (44). As such, they describe the equipotential sphere from its opposite sides, which is reflected by the inversion of their signs. The sides described in Eqs. (41) and (46) represent the side of the passive mass M_{BH} and active mass M , respectively, which can be observed by deriving Bekenstein’s entropy (44) based on Verlinde’s equation (46) (cf. Appendix 6). They are related (51) through the entropy variation sphere, which introduces the sign reversal. In such a radial configuration, a quantity is positive if it is consistent with the radius; else, it is negative. In particular, M_{BH} , M , R , and δR are parameters of this holographic 2-sphere. Moreover, R denotes a time independent version of δR , as discussed in the subsequent section.

7. Binary Potential and Binary Messages

Entropy is a measure of information (even if it is missing information [25]) and information is measured in bits. According to the holographic principle, the bounded interior and unbounded exterior are separated by a two-dimensional boundary, and by definition, each k^{th} bit is physically represented on this boundary (the holographic sphere A) by a unit Planck area [13, 18, 23]. For an area A , the boundary exhibits an information capacity of $N_A = A/\ell_P^2$ bits. However, this is an imprecise conclusion, considering $N_A \in \mathbb{R}$ and the number of bits is a natural number. Moreover, for a spherical surface, $A = 4\pi R^2$ N_A is a transcendental number: a quotient of the product of a transcendental number (π) with a rational number ($4R^2$) and a rational number (ℓ_P^2).

Therefore, the number of bits provided by the boundary is $[N_A] \in \mathbb{N}_0$. This is the floor function, that yields the greatest natural number less than N_A . Thus, the fractional part

$$0 < \{N_A\} < 1, \quad (52)$$

can be considered as a signature of the holographic sphere A . Perhaps the continuum hypothesis ensures a unique

$\{N_A\}$ for any given holographic sphere, regardless of the simultaneous existence of the same number of bits N_A on an infinitely countable number of other spheres.

Thus, the entropy variation (41) can be expressed as an information capacity of the holographic sphere A

$$\delta S = -\frac{ck_B}{2G\hbar} \delta\varphi N_A \ell_P^2 = -\frac{1}{2} k_B N_A \frac{\delta\varphi}{c^2}. \quad (53)$$

The 2nd term of (53) corresponds to ΔS [23, Eq. 3.12], where the Newton potential φ keeps track of the depletion of the entropy per bit on the holographic sphere A .

This equation can be further simplified by postulating the binary variational potential (or simply, binary potential) in Planck time t_P over the k -th Planck area ℓ_P^2 , defined as

$$\delta\varphi_k \doteq -\{0,1\} \ell_P^2 / t_P^2 = -\{0,1\} c^2. \quad (54)$$

This relationship between the speed of light and a Planck area is remarkable in the context of the recent discovery that Planck length and Planck time can be obtained from a Newtonian force-spring knowing only the value of the speed of light and with no knowledge of the gravitational constant G or Planck constant \hbar [26]. More specifically, the variational potential requires the notion of time, assumed as imaginary, i.e., $(ic)^2 = -c^2$. This unit also stems from the 2-dimensionality of the Planck area. Such a definition of the binary potential must be true if a bit of information is the only property of ℓ_P^2 on a holographic screen A . Therefore, the equipotential surface A and holographic screen A are the same 2-spheres.

By substituting Eq. (54) into Eq. (53), we obtain a binary variation of entropy on a holographic sphere A , given as

$$\delta S = -\frac{1}{2} k_B N_A \frac{\delta\varphi}{c^2} = -\frac{1}{2} k_B \sum_{k=1}^{\lfloor N_A \rfloor} \frac{\delta\varphi_k}{c^2} = \frac{1}{2} k_B N_1, \quad (55)$$

where the summation covers all the Planck areas of A , and $N_1 \in \mathbb{N}$ is the number of Planck areas with binary potential $\delta\varphi_k = -c^2$, further called ‘‘active Planck areas’’.

On comparing Bekenstein–Hawking entropy (44) with the binary variation of entropy (55), we get

$$S_{BH} = \delta S \Leftrightarrow \frac{1}{4} k_B N_{BH} = \frac{1}{2} k_B N_1 \Leftrightarrow N_1 = \frac{1}{2} N_{BH}, \quad (56)$$

which indicates that the temporary distribution of Planck areas on an event horizon can maximize the Shannon entropy. Therefore, the event horizon is an algorithmically random or patternless [27] binary message comprising a balanced number of Planck areas with binary potential (54) equal to $-c^2$ and 0.

An additional trivial observation is that the average potential of all the Planck areas on the event horizon is equal to the event horizon potential at a vertex, i.e.,

$$\frac{\sum_{k=1}^{N_1} (-c^2) + \sum_{k=1}^{\lfloor N_{BH} \rfloor - N_1} 0}{N_{BH}} = \frac{-N_1 c^2}{N_{BH}} = \frac{-\frac{1}{2} N_{BH} c^2}{N_{BH}} = -\frac{1}{2} c^2. \quad (57)$$

The two binary strings

$$X_1 = 11111111111111111111111111111111 \quad (58)$$

$$X_2 = 10110100101000101101 \quad (59)$$

assumed to be generated by tosses of a fair coin (random variable outcomes) must be considered equally random. However, based on the perspective of Kolmogorov complexity, the second string is more random than the first one considering it is a patternless binary sequence [27]. If strings (58) and (59) were messages transmitted bit by bit over a certain transmission channel, the probabilities for zero and one occurrences in the second message (59) would be equal ($p_0 = p_1 = 1/2$). Therefore the second message would be a noncompressible one, which maximizes the Shannon entropy, as

$$H(X_2) = -\frac{1}{2} \ln\left(\frac{1}{2}\right) - \frac{1}{2} \ln\left(\frac{1}{2}\right) = \ln(2), \quad (60)$$

expressed in nats, whereas the Shannon entropy of the message (58) is zero, as it could be compressed to just one bit. The maximal Shannon entropy of the second message (59) would also minimize the amount of energy required to erase a single bit of information on the event horizon, which is expressed using the Landauer erasure limit [28]

$$E_1 = T_{BH} k_B H(X_2) = T_{BH} k_B \ln(2). \quad (61)$$

On comparing the end terms of Eqs. (53) and (55), the variational potential can be expressed as

$$\delta\varphi = -\frac{N_1}{N_A} c^2, \quad (62)$$

which is an important relation that also (cf. Table 5) shows that the event horizon is a patternless binary message.

Considering the Hawking BH radiation is a diameter-dependent black-body radiation (27) bearing no information regarding BH interior conditions, it is a patternless message containing the same number of zeros and $-c^2$ terms ($-c^2/2$ on average), as a binary one-time pad secret key. Holographic screens other than event horizons provide more diversified (and less surprising) distributions of zeros and ones with lower Shannon entropies (further discussed in Section 9). However, an event horizon is a patternless binary message (59) and the quantum information of the in-fallen matter cannot be hidden in correlations between the semiclassical Hawking radiation and the *internal states* of the BH, as asserted by the no-hiding theorem [1].

The entropic work on a BH event horizon using the Hawking temperature (40) and Bekenstein–Hawking entropy (44) can be expressed as

$$T_g \cdot \delta S = \left(\frac{\hbar}{2\pi c k_B} \frac{GM_{BH}}{R_{BH}^2} \right) \left(\frac{k_B N_{BH}}{4} \right) = \frac{M_{BH} c^2}{2} = \frac{d_{BH} E_P}{8}, \quad (63)$$

which differs from the BH mass–energy equivalence

$$E_{BH} = M_{BH} c^2 = \frac{1}{4} d_{BH} E_P, \quad (64)$$

where E_p is the Planck energy, and results in two distinct Landauer bounds on a minimum BH information capacity (cf. Appendix 7): $N_{BH} = 2\ln(2)$ (mass–energy equivalence, 1 bit) and $N_{BH} = 4\ln(2)$ (BH entropic work, 2 bits). To assign one unit of entropy on a BH horizon at least four bits (Planck areas) are required.

Heisenberg’s Uncertainty Principle (HUP) is commonly expressed as

$$\delta P \delta R \geq \hbar/2, \quad (65)$$

where δP is momentum and δR is the position uncertainty. In an alternative form, the above equation can be expressed as

$$\delta E \delta t \geq \hbar/2, \quad (66)$$

where δE is energy and δt is the time uncertainty. According to the equipartition theorem, the energy uncertainty δE must be at least the energy of one bit ($\delta E \geq k_B \delta T/2$). Substituting this with $\delta t = t_p$ into Eq. (66) we get the temperature uncertainty

$$\delta T = T_p, \quad (67)$$

which is equal to the Planck temperature. Therefore, temperature uncertainty δT equals the Planck temperature if time uncertainty δt equals Planck time.

The nontrivial BH microstate degeneracy starts at 3 vertices [29] of the Voronoi triangulation corresponding to the Delaunay triangulated π -bit BH with 4 vertices (Fig. 3(a)). This is interesting in context of the equipartition theorem for an atom in a monatomic ideal gas, that — assuming that the atom exhibits π degrees (bits) of freedom, instead of three — can be defined as

$$E = \frac{\pi}{2} k_B T. \quad (68)$$

This form enables the recovery of the exact (not approximate) Unruh (38) and Hawking (39) temperature equations with the derivations presented in [31] if energy uncertainty δE is interpreted in terms of temperature uncertainty δT . Notably, equipartition theorem is rigorously proven only for a single degree of freedom (one bit), and the energy (68) corresponds to the π -bit BH, as revealed by substituting BH mass–energy equivalence (64) along with (11) into (68).

Based on the Planck–Einstein (or Compton wavelength) relationship

$$\delta E = h \delta \nu = \frac{2\pi \hbar c}{\delta \lambda}, \quad (69)$$

where the uncertainty of energy δE is expressed as the uncertainty of wavelength $\delta \lambda$ the HUP (66) is expressed as

$$\delta \lambda \leq 4\pi c \delta t \quad (l \leq 4\pi t). \quad (70)$$

Alternatively, the mass–energy equivalence $\delta E = \delta M c^2$ can be used to replace energy uncertainty with mass uncertainty δM , and set $c = \delta R/\delta t$ [31] to express HUP (66) as

$$\delta M \delta R \geq \hbar/2c. \quad (71)$$

On substituting $\delta M = 2\pi \hbar/(c \delta \lambda)$ (Compton wavelength of δM) into (71), we get

$$\delta \lambda \leq 4\pi \delta R \quad (l \leq 2\pi d), \quad (72)$$

which also supports the finding that for $\delta \lambda \geq \ell_p$ ($l \geq 1$) (4), $d_{BH} \geq 1/(2\pi)$ sets a minimum BH Planck temperature T_p (11). Moreover, by substituting $\delta M = \delta R c^2/2G$ (Schwarzschild mass corresponding to δR) into (71), we can recover the Planck length [31] as the minimum BH radius, expressed as

$$\delta R^2 \geq \ell_p^2, \quad c^2 \delta t^2 \geq \ell_p^2, \quad (73)$$

and hence, the Planck time t_p can be considered as the minimum time period δt on a BH horizon.

In this section, we introduced the concept of the disturbing time period δt and equated it with time uncertainty. Although, we implicitly equated the position uncertainty with the disturbing δR (31) or BH radius R_{BH} (26) (as shall be discussed later, they are additive inverses of each other), it is irrelevant in the current context because the uncertainties in HUP are always nonnegative. These aspects are further discussed in Section 9.

Micro-BHs are inherently unstable and prone to collapses [20]. The HUP, BH geometry, and information theory further deliver arguments in support of this claim. In particular, the BH temperature limit (67) emerges from the HUP yielding $d_{BH} = 1/(2\pi)$, whereas $d_{BH} = 1/\sqrt{\pi}$ provides one Planck area (one bit). At least four vertices — the fundamental requirement for defining the event horizon (13) — are given for $d_{BH} = 1$. Moreover, the imaginary time period is exhibited by BH with $d_{BH} = \sqrt{2}$ (103). Twelve Planck areas (with only one precise diameter) correspond to the BH with $d_{BH} = 2$, which is also recovered from the HUP (73). Compared to 7.88E90 Planck areas (Sagittarius A*), the maximization of Kolmogorov complexity of a BH binary message (59) comprising 20 Planck areas is much more challenging.

Generally, the radius of a BH event horizon R_{BH} is derived as a singularity of the Schwarzschild metric, which yields an exact solution to the Einstein field equations without the cosmological constant Λ , thereby describing the gravitational field outside a spherical, uncharged, and nonrotating mass. Note that the cosmological constant introduces concepts like dark matter or dark energy, which are redundant in the framework of Verlinde’s entropic gravity [23]. More specifically, the Schwarzschild metric has two singularities: at $R = 0$ ($R = 0$ is always singular in polyspherical coordinates) and at $R = R_{BH}$.

However, R_{BH} is also a solution of the escape velocity threshold, as follows

$$v_E^2 = \frac{2GM}{R} \leq c^2, \quad \frac{GM}{R_{BH}} = \frac{1}{2} c^2. \quad (74)$$

Therefore, by equating the variational potential (50) with the binary potential (54), we can determine the relationship between the mass M and radius δR . This can be

conducted for $\delta\phi_k = -c^2$ (it is undefined for $\delta\phi_k = 0$) resulting in

$$\delta R_1 = \frac{GM}{c^2}, \quad (75)$$

which represents half the Schwarzschild radius δR_{BH} of mass M and equals Planck length if M is equal to Planck mass. Therefore, we recovered the orbital velocity threshold w.r.t. δR_1 , as follows

$$v_o^2 = \frac{GM}{\delta R_1} \leq c^2, \quad (76)$$

which expresses the second (or rather, the first) significant velocity related to mass M . This is meaningless in context of the Schwarzschild metric, as it simply does not encompass orbital velocity (although it encompasses the photon-sphere radius $R_p = 3GM/c^2$). Orbital velocity is included in the Kerr metric, which is another exact solution to the Einstein field equations without the cosmological constant and acts as a generalization of the Schwarzschild metric to the gravitational field prevailing outside a spherical and uncharged mass, rotating with an angular momentum J . In contrast, Birkhoff's theorem asserts that a spherically symmetric solution to Einstein's equations in the vacuum must necessarily be static, and the exterior solution must be described by Schwarzschild metric in the absence of the cosmological constant [32].

Interestingly, for constant M , a hypothetical 2-sphere of radius δR_1 (75) comprises the same number of bits as given by Bekenstein's entropy (44) (using (2))

$$\begin{aligned} N_{BH} &= 4\pi \frac{4G^2 M^2}{c^4} \frac{c^3}{\hbar G} = 16\pi m^2 \\ N_{\delta R_1} &= 4\pi \frac{G^2 M^2}{c^4} \frac{c^3}{\hbar G} = 4\pi m^2 = \frac{1}{4} N_{BH} \end{aligned} \quad (77)$$

Furthermore, by equating Verlinde's entropic formula (46) (2nd term) with (53) (2nd term), we can express the variational potential (50) on the entropy variation sphere as a function of the information capacity N_A of the sphere and the reduced Compton wavelength of mass M , given as

$$\delta\phi = -\frac{4\pi c^2}{N_A} \frac{\delta R}{\lambda_M}. \quad (78)$$

Thus, combining (78) with the variational potential (50) (2nd term), we get

$$N_A = \frac{4\pi\delta R^2}{\ell_p^2}, \quad \text{and since,} \quad N_A = \frac{4\pi R^2}{\ell_p^2}, \quad (79)$$

we conclude that both δR and R provide the same information capacity N_A on the spherical screen A . However, δR is related to the notion of the time period δt (31), whereas R is not. Thus, we conclude that $R^2 = \delta R^2$. Additionally, δR is an additive inverse of R , as discussed in the subsequent section.

8. Inertial Potential

Here, we introduce the concept of inertial potential of the active mass M , such that

$$\phi_a = \frac{GM}{R}, \quad (80)$$

is an additive inverse of this mass gravitational potential, and is considered an equivalent to the latter. Indeed, the gravitational field and inertia are physically equivalent (equivalence principle), wherein the inertia originates through interactions between all masses in the universe (Mach's principle) on which principles the theory of relativity is based [33]. Potential ϕ relates the notions of mass and space, similar to mass density ρ , Schwarzschild radius (26), or the uncertainty principle.

Based on the definition of binary potential (54), we observed that radius R emerges as irrelevant in the inertial potential (80). By introducing the inertial potential gradient (83) into the Unruh temperature (38) substituting it along with the binary variation of entropy (55) and the radius of the holographic sphere $R^2 = N_A \ell_p^2 / 4\pi$ in Eq. (43) we obtain the entropic work (using (62) in the last term), given as

$$\begin{aligned} F \circ \delta R &= T_a \cdot \delta S = \frac{\hbar}{2\pi c k_B} \left(-\frac{GM}{R^2} \right) \cdot \left(\frac{1}{2} k_B N_1 \right) = \\ &= -\frac{\hbar G}{4\pi c} M \frac{4\pi}{N_A \ell_p^2} N_1 = -\frac{N_1}{N_A} M c^2 = M \delta\phi \end{aligned} \quad (81)$$

whose modulus attains equilibrium (56) at the event horizon. Therefore, mass M represents the proportionality constant, similar to that in Isaac Newton's second law of motion, and the actual radius R of our toy universe, portrayed in Fig. 6, is irrelevant in our considerations.

The supermassive BH Sagittarius A* has an estimated mass $M_{BH} \approx 8.62E36$ kg, yielding diameter $D_{BH} \approx 2.56E10$ m. The BH surface gravity can be expressed as⁵

$$g_{BH} = \frac{GM_{BH}}{R_{BH}^2} = \frac{c^2}{D_{BH}}, \quad (82)$$

which is independent of the gravitational constant G .

This is an extremely large value, even for supermassive BHs. For the BHs listed in Table 1, g_{BH} displays an order of magnitude of Planck acceleration $a_p = \sqrt{c^7/\hbar G} = 5.56E51$ m/s², attained by the π -bit BH. For Sagittarius A*, this is still $\sim 3.51E6$ m/s². A BH with g_{BH} equal to the Earth's surface gravity (9.98 m/s²) would require a diameter of $D_{BH} = 9E15$ m, which is slightly less than one light year.

Such large black holes are not observed in nature.

Thus, any inertial acceleration of an object heavier than the threshold of distinguishability (6) can be considered to be lower than a BH surface gravity. The inertial

⁵ $g = 1/d$, where g is Planck acceleration multiplier.

acceleration a denotes the gradient of inertial potential (80), such that

$$a = \nabla_R \phi_a = -\frac{GM}{R^2} < \frac{c^2}{2R_{BH}}, \quad (83)$$

thereby indicating that the inertial potential of such a mass M at $R_{BH} = R$ (80) must be greater than the BH potential of $-c^2/2$

$$\phi_a = \frac{GM}{R} > -\frac{1}{2}c^2. \quad (84)$$

This is an important finding, since it signifies that the inertial potential of such a mass always describes a non-equilibrium situation, where the equilibrium is defined by the BH thermodynamic equilibrium (56) and the Laplace's (28) or Poisson's (29) equation.

Similarly, we presume that the variational potential (50) should be higher than the BH potential, expressed as

$$\delta\phi \doteq -\frac{GM}{\delta R} > -\frac{1}{2}c^2. \quad (85)$$

Since in this case mass M is away from the equilibrium (56), we obtain

$$\delta R > \frac{2GM}{c^2}, \quad (86)$$

which indicates that the disturbing radius δR , wiggling mass M against the Poisson's equation (29) must be larger than the Schwarzschild radius (26) of mass M . If M is a BH, it cannot be wiggled, as this would invalidate the BH equilibrium (56) condition and Bekenstein's threshold (44) on a BH entropy. The disturbing radius δR should be larger than the Planck length (73).

Based on Eqs. (79), (81), (84), and (85), we can conclude that the variation potential (50) represents the gravitational potential corresponding to the inertial potential (80), i.e.

$$\delta R \geq \ell_p, \quad \delta R^2 = R^2, \quad \delta R = -R, \quad \delta\phi = \phi_a, \quad (87)$$

as shown in Fig. 7.

The variational potential (78) induced by wiggling the location of the test mass M must be equal to the BH potential of $-c^2/2$, assuming that the test mass M could be wiggled on a BH horizon. Thus, according to Eq. (87),

$$\delta\phi = -\frac{4\pi c^2}{N_A} \frac{\delta R^{BH}}{\lambda_M} = \frac{4\pi c^2}{N_{BH}} \frac{R_{BH}}{\lambda_M} \doteq -\frac{c^2}{2}. \quad (88)$$

In this case, a simple calculation (cf. Appendix 8) revealed that the Compton wavelength of the active mass M in (88) is the additive inverse of the BH Compton wavelength (9), corresponding to the BH mass required to be emitted to ensure its total collapse (20), given as

$$\lambda_M^{BH} = -\frac{2\ell_p^2}{R_{BH}} = -\lambda_{BH}. \quad (89)$$

This is not surprising, considering M exhibits an ultimately attained equilibrium (56), and hence, becomes a portion of BH. However, this is negative because M was introduced to M_{BH} in a direction opposite to its radius.

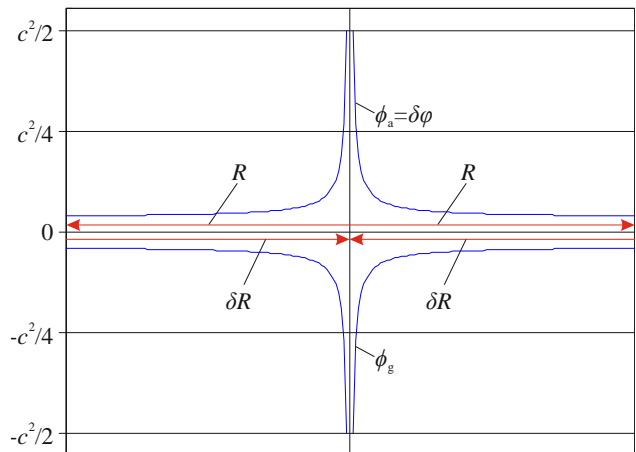


Fig. 7: Gravitational, inertial, and variational potentials (not to scale).

In a subsequent section, we shall investigate the meaning of time period δt and the distance δL tangential to the holographic sphere A .

9. Imaginary Time and Kinematics on Holographic Spheres

Let us postulate the velocity v_R as normal to a holographic sphere, and thus, unobservable. Evidently, only one axis is normal to this sphere at each Planck area, whereas the number of tangential axes is infinite. Let us further postulate that this unobservable velocity v_R is bounded with the classical observable velocity

$$v = \frac{\delta L}{\delta t}, \quad (90)$$

where δL denotes a certain length, orthogonal to the disturbing radius δR (and by equation (87) orthogonal to this sphere radius R) based on the Pythagorean relation

$$v^2 + v_R^2 = c^2. \quad (91)$$

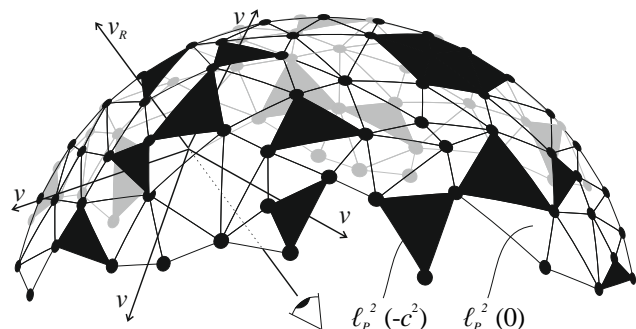


Fig. 8: Simplified illustration of visual perception of movement on a holographic sphere (not to scale).

We assumed that δL is observable as moving on the screen owing to the varying Planck areas with their binary potentials (54), as schematically shown in Fig. 8. Contrary to an interior-less BHs, each observer is bounded within $(2+i)$ -dimensional sphere A , with two spatial dimensions encoding its information capacity N_A with $[N_A]$

triangular Planck areas and imaginary time, whereas $0i = 0$ denotes the present moment of perception (observation), wherein an active Planck area can become inactive, and vice versa. However, we do not investigate the precise mechanism of this process. It is known that the photoisomerization of a photon in a cone cell of the eye cascades signal transduction.

Based on this postulate (91), the Lorentz factor can be derived as

$$\gamma = \left(1 - \frac{v^2}{c^2}\right)^{-\frac{1}{2}} = \frac{c}{v_R}, \quad (92)$$

the Lorentz contraction (squared) becomes ($0 \leq \delta L^2 \leq \delta L_0^2$)

$$\delta L^2 = \delta L_0^2 \left(1 - \frac{v^2}{c^2}\right) = \delta L_0^2 \frac{v_R^2}{c^2}, \quad (93)$$

and time dilation (squared) becomes ($0 \leq \delta t_0^2 \leq \delta t^2$)

$$\delta t^2 = \delta t_0^2 / \left(1 - \frac{v^2}{c^2}\right) = \delta t_0^2 \frac{c^2}{v_R^2}. \quad (94)$$

Overall, the simple forms of these equations endorse the validity of the postulate (91).

According to Eqs. (38)–(40), the observable acceleration

$$a = \frac{\delta R}{\delta t^2}, \quad (95)$$

is perpendicular to the holographic sphere. Additionally, the application of the disturbing radius δR (31) and disturbing time period δt in observable acceleration a is justified by our previous conclusion (85) that any inertial acceleration introduces a nonequilibrium condition.

Let us then postulate that this observable acceleration a is, similarly to velocity (91), bounded with a certain unobservable orthogonal acceleration a_T , which is tangential to the holographic sphere at a given Planck area, based on the similar Pythagorean relation

$$a_T^2 + a^2 = a_P^2 = \frac{c^2}{t_P^2} = \frac{\ell_P^2}{t_P^4}. \quad (96)$$

Moreover, a (95) can be expressed using Unruh temperature (38) as

$$a = \frac{2\pi c k_B}{\hbar} T_a = 2\pi a_P \frac{T_a}{T_P}. \quad (97)$$

Substituting Eq. (97) it into Eq. (96) we get

$$a_T = a_P \sqrt{1 - 4\pi^2 \tau^2}, \quad (98)$$

where

$$\tau = \frac{T_a}{T_P} = \frac{1}{2\pi} \frac{a}{a_P} \leq 1 \quad \tau \in \mathbb{R}, \quad (99)$$

denotes the ratio of Unruh temperature or acceleration to the Planck temperature or acceleration. If $\tau = 1/(2\pi)$, $a_T = 0$ and the only radial acceleration a is equal to the Planck acceleration, a_P exists on the holographic sphere, which represents the Big Bang condition. If $\tau = 0$ (absolute zero), then $a_T = a_P$ and the radial acceleration a vanishes in (96).

At a BH horizon with $\tau_{BH} = 1/(2\pi d)$ (11), (98) reduces into

$$a_T^{BH} = a_P \sqrt{1 - \frac{1}{d^2}}, \quad (100)$$

which is imaginary if $d^2 < 1$. The real values of a_T were first produced with the π -bit BH ($d_{BH} = 1$) with surface gravity (82) equaling to Planck acceleration, which also validates the proposed postulate (96).

Moreover, the Unruh temperature (38) can be expressed as

$$T_a = \frac{\hbar}{2\pi c k_B} \frac{\delta R}{\delta t^2} = \frac{r_\delta}{2\pi t^2} T_P, \quad (101)$$

where $\delta R = r_\delta \ell_P$, $\delta t = t t_P$, $r_\delta \in \mathbb{R}$, and $t \in \mathbb{R}$ denote the Planck length and time multipliers in δR and δt . At a BH horizon, this temperature must be equal to the BH temperature (11), which results in the following with (87) (thus, the sign is reversed; $r_\delta = -r_{BH}$):

$$\frac{r_\delta^{BH}}{2\pi t^2} = \frac{1}{2\pi d_{BH}}, \quad r_\delta (-2r_\delta)^{BH} = t^2, \quad \frac{\delta R^2}{\delta t^2}^{BH} = -\frac{1}{2} c^2. \quad (102)$$

This is equal to the BH potential (27). Since δR is real, we conclude that at a BH horizon time period δt is imaginary

$$\frac{\delta R}{\delta t}^{BH} = \frac{i}{\sqrt{2}} c, \quad \delta t = \frac{i D_{BH}}{c \sqrt{2}}, \quad (103)$$

and that the unobservable velocity v_R is also imaginary and can be expressed as real

$$v_R = \frac{\delta R}{\delta t_R} = \frac{\delta R}{i \delta t}, \quad (104)$$

upon the introduction of the complementary time period δt_R related to the *classical* time period δt based on integral powers of i

$$\delta t_R = i \delta t, \quad \delta t_R^2 = -\delta t^2, \quad \delta t_R^3 = -i \delta t^3, \quad \delta t_R^4 = \delta t^4. \quad (105)$$

Thus, at the BH horizon, Eqs. (103) and (104) can be combined to derive

$$v_R^2 = \frac{\delta R^2}{\delta t_R^2}^{BH} = \frac{1}{2} c^2, \quad (106)$$

which represents the inverse of a BH potential (27), and using (91) provides the observable velocity of

$$v^2 = \frac{\delta L^2}{\delta t^2}^{BH} = \frac{1}{2} c^2. \quad (107)$$

Substituting $\delta t = it_p$, the shortest theoretically measurable time period, into (103) yields $d = \sqrt{2}$, which is the minimum BH diameter multiplier allowing for the notion of (imaginary) time.

Furthermore, Eqs. (102) and (103) yield the acceleration as an additive inverse of the BH surface gravity (82):

$$a = \frac{\delta R}{\delta t^2} \stackrel{BH}{=} -\frac{c^2}{2\delta R} = \frac{ic}{\sqrt{2}\delta t}, \quad (108)$$

which is congruent with (87).

Based on Eq. (104), time dilation (94) can be expressed as

$$\frac{\delta R^2}{\delta t_0^2} = -c^2, \quad (109)$$

which becomes independent both on the time period δt measured in a moving inertial frame of reference and the velocity v of this frame. The velocity bound (91) and Lorentz contraction (93) results in (cf. Appendix 12)

$$\frac{\delta L_0^2}{\delta L^2} + \frac{\delta L^2}{\delta R^2} = 1, \quad (110)$$

which is neither the time period nor velocity dependent.

Let us now postulate that the unobservable acceleration can presume the form of

$$a_T = \frac{\delta L}{\delta t_R^2}. \quad (111)$$

The current conclusions concerning the velocities (90) and (104) and accelerations (95) and (111) are implied by Mach's principle: observable velocity provides information on a holographic sphere, whereas observable acceleration acts on the holographic sphere and is originated in an interaction between all masses in the universe. To illustrate this principle, we quote Steven Weinberg: "There is a simple experiment that anyone can perform on a starry night, to clarify the issues raised by Mach's principle. First stand still, and let your arms hang loose at your sides. Observe the stars are more or less unmoving, and that your arms hang more or less straight down. Then pirouette. The stars will seem to rotate around the zenith, and at the same time your arms will be drawn upward" [34]. The questions that arise are, why do one's arms hang loose when the stars are still, and why they would be drawn upward when the stars rotate. The most important factor for our definitions of the observable velocity (90), acting tangential to the holographic sphere, and the observable acceleration (95), acting perpendicularly to it, is that the *stars* made to whirl around the person standing in the center of a planetarium would not draw the person's arms upward.

The bounds of velocity (91) and acceleration (96) can now be expressed in terms of δt , using (105) as

$$\frac{\delta L^2}{\delta t^2} + \frac{\delta R^2}{\delta t_R^2} = \frac{\delta L^2}{\delta t^2} - \frac{\delta R^2}{\delta t^2} = c^2, \quad (112)$$

$$\frac{\delta L^2}{\delta t_R^4} + \frac{\delta R^2}{\delta t^4} = \frac{\delta L^2}{\delta t^4} + \frac{\delta R^2}{\delta t^4} = a_p^2 = \frac{c^2}{t_p^2}. \quad (113)$$

Eq. (112) was divided by δt^2 and both these equations were added to derive at the relationship:

$$\delta L^2 = \frac{1}{2} \delta t^2 (a_p^2 \delta t^2 + c^2), \quad (114)$$

bounding δt with δL . Equations (91) and (96) can be expressed in terms of δt_R , obtaining the bound for δR as

$$\delta R^2 = \frac{1}{2} \delta t^2 (a_p^2 \delta t^2 - c^2), \quad (115)$$

which considered in combination yields

$$\delta L^2 + \delta R^2 = a_p^2 \delta t^4, \quad (116)$$

corresponding to (96) with substituted (105). Discretized by the Planck length and time for natural multipliers r , t , a , this represents the OEIS A349078 sequence.

As observed, δL and δR are bounded by the Pythagorean (circle) relation (116) and by the hyperbolic relation:

$$\delta L^2 - \delta R^2 = c^2 \delta t^2, \quad (117)$$

as shown in Fig. 9.

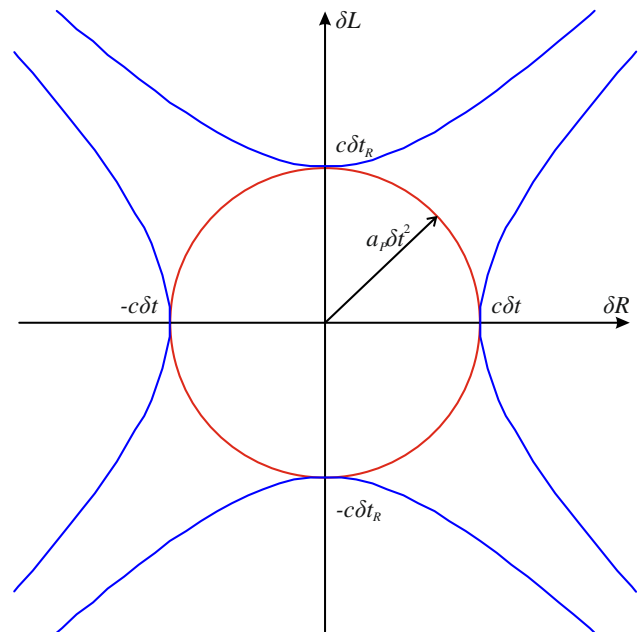


Fig. 9: Pythagorean (red) and hyperbolic (blue) relations between δL perpendicular to the disturbing radius δR .

Dividing Eqs. (114) and (115) with $\delta t^2 \neq 0$, we get

$$\frac{\delta L^2}{\delta t^2} = \frac{1}{2} c^2 (t^2 + 1) = v^2 \leq c^2, \quad (118)$$

and

$$\frac{\delta R^2}{\delta t^2} = \frac{1}{2} c^2 (t^2 - 1) = -v_R^2 \leq c^2. \quad (119)$$

Considering, no velocity exceeds the speed of light c , the bounds are set on inequalities (118) and (119), as

listed in Table 4. Based on the BH bounds (106) and (107), we can conclude that

$$0 \leq \frac{\delta L^2}{\delta t^2} \leq \frac{1}{2}c^2, \quad 0 \leq \frac{\delta R^2}{\delta t^2} \leq \frac{1}{2}c^2. \quad (120)$$

Table 4: Characteristic Planck time multipliers

	0	$c^2/2$	c^2
$\delta L^2/\delta t^2$	$t^2 = -1$	$t^2 = 0$	$t^2 = 1$
$\delta R^2/\delta t^2$	$t^2 = 1$	$t^2 = 2$	$t^2 = 3$

On substituting Eqs. (118) and (119) into the orbiting condition $v_O^2 \leq v^2 \leq v_E^2$, with (76) and (74) we get

$$\frac{R_{BH}}{R} \leq t^2 + 1 \leq \frac{2R_{BH}}{R}, \quad (121)$$

and

$$\frac{R_{BH}}{R} \leq t^2 - 1 \leq \frac{2R_{BH}}{R}. \quad (122)$$

These are interesting results. Our toy universe, shown in Fig. 6, contains a black hole in its center. But it is not necessary for the above relations to be valid. The Schwarzschild radius of the Sun (2E30 kg), for example, amounts to $R_{BH} = 2953.34$ m.

At BH horizon $R = R_{BH}$, and hence, $0 \leq t^2 \leq 1$ and $2 \leq t^2 \leq 3$ in Eqs. (121) and (122), which corresponds to the $c^2/2$ to c^2 range in Table 4. Furthermore, we observed that the range 0 to $c^2/2$ in Table 4 is achieved by $0 \leq t^2 + 1 \leq 1$ ($-1 \leq t^2 \leq 0$) and $0 \leq t^2 - 1 \leq 1$ ($1 \leq t^2 \leq 2$) with a gap $0 \leq t^2 \leq 1$. Comparing this with Eqs. (121) and (122), we can conclude that maximum significant BH radius equals $2R_{BH}$. Notably, there are no celestial objects other than BHs⁶ having a potential equal or lower than $|-c^2/4|$. For a constant $M_{BH} = R_{BH}c^2/2G$ and $R_{MAX} = 2R_{BH}$ the Bekenstein bound [18] yields twice BH entropy (44) (M_{BH} is bounded by R_{BH} but R varies)

$$\begin{aligned} S &\leq \frac{2\pi k_B c R_{MAX} M_{BH}}{\hbar} = 2\pi k_B r_{MAX} m_{BH} = \\ &= \frac{2\pi k_B c 2R_{BH}}{\hbar} \frac{R_{BH} c^2}{2G} = \frac{1}{2} k_B N_{BH} = k_B N_1 \end{aligned} \quad (123)$$

which also according to Eq. (56) equals the number of active Planck areas on a BH horizon. We can express the radius R_k of a holographic sphere of a constant mass $M = mm_p$, $m \in \mathbb{R}$ as a function of GM/c^2 multiplier $k \in \mathbb{R}$, as

$$R_k = k \frac{GM}{c^2} = km\ell_p, \quad (124)$$

which corresponds to the Schwarzschild radius (26) of mass M for $k = 2$. This yields potential $\phi_g(R_k)$ (25) and the number of the active Planck areas (62) at the holographic sphere of radius R_k equal to $N_1 = N_A/k$. Therefore, there

⁶ Even white dwarfs (such as Sirius; $M = 4.1E30$ kg, $R = 1.19E9$ m $\rightarrow \phi_g = -2.3E11$ m²/s²) and neutron stars (such as PSR J0740+6620; $M = 4.14E30$ kg, $R = 1.5E4$ m $\rightarrow \phi_g = -1.83E16$ m²/s²) provide potential lower (up to modulus) than BHs, with the latter being close to $-c^2/4 = -2.25E16$ m²/s².

are less active Planck areas *outside* the BH horizon of mass M than $N_1 = N_A/2$.

From Eqs. (62) and (124), we have recovered (56) without the use of Bekenstein-Hawking entropy (44).

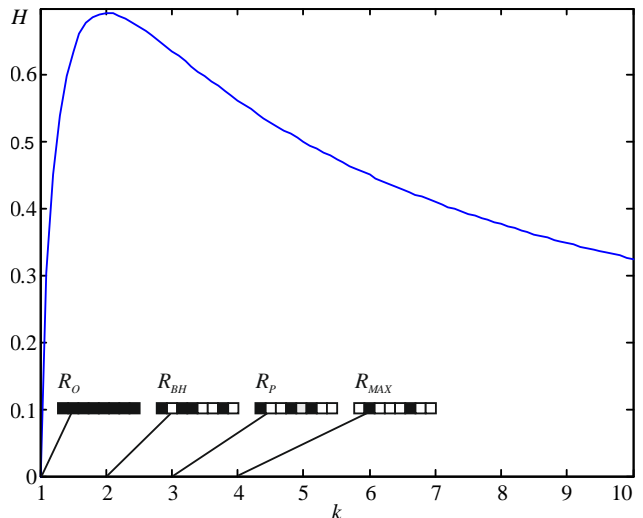


Fig. 10: Shannon entropy (in nats) of holographic spheres, as a function of GM/c^2 multiplier k ; $M = \text{const}$.

Substituting G from ℓ_p^2 , (124) we get

$$Mc \frac{\ell_p^2}{R_k} = \frac{\hbar}{k}, \quad (125)$$

which for $k = 2$ corresponds to HUP bound (65). Parameters of the holographic spheres of a constant mass M are listed in Table 5, while Fig. 10 shows their BH binary Shannon entropy (60) (cf. Appendix 14)

$$H(k) = \ln(k) - \frac{k-1}{k} \ln(k-1). \quad (126)$$

Obviously $R_{MIN} = 0$ and R_O have no physical meaning.

Substituting δR^2 from time dilation (109) into Eq. (119), we get

$$t^4 - t^2 - 2t_0^2 = 0, \quad (127)$$

where the proper time is $\delta t_0 = it_0 t_p$ and $t_0 \in \mathbb{R}$ represents the Planck time multiplier. Subsequent t_0^2 from a set of triangular numbers (0, 1, 3, 6, ...; OEIS A000217) substituted into $t^2 = 1 \pm \sqrt{1+8t_0^2}$ (127) yield subsequent nonpositive $t^2 = 0, -1, -2, -3, \dots$ and positive $t^2 = 1, 2, 3, \dots$ squares of Planck time multipliers.

An outstanding property of Boolean $\{0, 1\}^N$ address space is that the mean Hamming distance between any address a_m and all the other addresses (including a_m) is $N/2$, whereas the variation is $N/4$ [35]. If an $\{N\}$ -cube [3] was inscribed in the closed N -ball most of its vertices would lay at or near the equator, whereas the unit of the active Planck area ($-c^2$) suggests particular orientation of BH address space, with vertex 000... representing one pole and vertex 111... [$-c^2$] representing the other pole. This indicates a link between diameter only dependent Planck BH blackbody spectral radiance (130), (131) and the corresponding patternless BH binary message (59). Interestingly the number of available BH horizon ar-

rangements comprising $N_1 = N_{BH}/2$ active Planck areas with binary potential (54) equal to $-c^2$ decreases from 50% (2-bit BH) with N_{BH} . Using Stirling's approximation for large N_{BH} it amounts

$$\left(\frac{N_{BH}}{N_1}\right) / 2^{N_{BH}} \approx \sqrt{\frac{2}{\pi N_{BH}}} = \frac{\sqrt{2}}{\pi d_{BH}}. \quad (128)$$

A relation between a bit of a binary message (58) and a wavelength multiplier l requires further research. It is certainly easier to maintain patternlessness of a longer binary message, which is likely to be responsible for a flatter spectral radiance of larger BHs, such as Sagittarius

Table 5: Size (R, D, d), potential (ϕ_g), information capacity (N_A), no. and probability of occurrence of active Planck areas (N_1) within all Planck areas (N_A), Bekenstein bound (S/k_B), and Shannon entropy (H) of holographic spheres for a constant mass $M = m m_p$, $m \in \mathbb{R}$, $k \in \mathbb{R}$.

R	$R_{MIN} = 0$	$R_O = m\ell_P$	$R_{BH} = 2m\ell_P$	$R_P = 3m\ell_P$	$R_{MAX} = 4m\ell_P$	$R_k = km\ell_P$
D	$D_{MIN} = 0$	$D_O = 2m\ell_P$	$D_{BH} = 4m\ell_P$	$D_P = 6m\ell_P$	$D_{MAX} = 8m\ell_P$	$D_k = 2km\ell_P$
$\phi_g = -GM/R$	$-\infty$	$-c^2$	$-c^2/2$	$-c^2/3$	$-c^2/4$	$-c^2/k$
$d = D/\ell_P$	0	$2m$	$4m$	$6m$	$8m$	$2km$
$N_A = \pi d^2$	0	$4\pi m^2$	$16\pi m^2 = N_{BH}$	$36\pi m^2$	$64\pi m^2$	$4\pi k^2 m^2$
$N_1 = -\phi_g N_A / c^2$	0	$4\pi m^2 = N_{BH}/4$	$8\pi m^2 = N_{BH}/2$	$12\pi m^2 = 3N_{BH}/4$	$16\pi m^2 = N_{BH}$	$4\pi k m^2$
$p_1 = N_1/N_A$	0	1	$1/2$	$1/3$	$1/4$	$1/k$
S/k_B (rel. to M)	0	$N_{BH}/8 = N_1/4$	$N_{BH}/4 = N_1/2$	$3N_{BH}/8 = 3N_1/4$	$N_{BH}/2 = N_1$	$kN_{BH}/8 = 2\pi k m^2$
$H(N_1/N_A)$	0	0	$\ln(2)$	$\ln(3) - 2\ln(2)/3$	$\ln(4) - 3\ln(3)/4$	$\ln(k) - (k-1)\ln(k-1)/k$

Certain dynamics scenarios can be contemplated in the simplified model of a spherical universe with two masses (Fig. 6), as shown in Fig. 11. The scenarios involving more than two bodies are not discussed, as they are irrelevant. In any given moment of perception, only two bodies interact with each other through the Planck area ℓ_P^2 in the Planck time t_P , and exchange the information in units of 0 or $-c^2$ according to the second law of Newton (47) and Newton's law of gravity (48).

The mass M in a state of a timeless free fall on M_{BH} is shown in Fig. 11(a), where $\delta R = 0$. Therefore, no entropic work occurs, and the system is entirely described by the Poisson's equation (29) with the inhomogeneity of the mass density included in the $4\pi G\rho$ term. This equation is independent of time or the variations of other quantities (position, velocity) with time. In particular, $\delta\varphi$ is infinite (50) and $A = 0$ for vanishing δR ; therefore, the variation of entropy δS is zero (41), such as that in the limiting case of the binary Shannon entropy (for $p_0 = 0$ or $p_1 = 0$), where $0\ln(0)$ is defined as 0.

The entropic work is shown in Fig. 11(b–d). The notion of time emerges from the instantaneous variations of entropy (41) induced by the instantaneous variations of δR in time δt (31).

As shown in Fig. 11(b), the mass M moves along a spiral trajectory towards M_{BH} . Obviously the geometry of this trajectory is not described in Fig. 11(b). While the variations of entropy δS (41) is defined and nonvanishing ($\delta R \neq 0$ and $\delta R/\delta t \neq 0$), the velocity of M is below the orbital velocity v_O defined by M_{BH} and R ($M \ll M_{BH}$). Consequently, a holographic 2-sphere A emerges both as the gravitational potential (25) sphere and entropy variation sphere (50). Subsequently, as time progresses, the system aims toward the equilibrium (56), $N_1(t) \rightarrow N_{BH}(t)/2$.

A^* (cf. Appendix 13). Neutron stars and white dwarfs supported against collapse owing to Pauli exclusion principle, also emit blackbody radiation. Therefore, they generate patternless binary messages. Perhaps, just one spherical side of BHs hints their anyonic nature, whereas neutron stars and white dwarfs exhibit fermionic natures.

These considerations are not surprising. We observed and modeled a BH as a 2-sphere, from which the electromagnetic radiation cannot escape. However, in the context of the graph of nature, the BH is a patternless binary message. Both δt and δt_R are imaginary and become real ($0i = 0$) only at the moment of interaction/observation of the Planck area ℓ_P^2 at the holographic sphere.

As shown in Fig. 11(c), the velocity of M is greater than the orbital velocity v_O and less than the escape velocity v_E . Therefore, M orbits surrounding M_{BH} . If the entropic work is being done, $\delta R \neq 0$ and $\delta R/\delta t \neq 0$, which implies fluctuations in the instantaneous velocity of an orbiting body ranging between the orbital and escape velocities. In this case, $N_1(t) < N_A(t)/2$ and the structure of M and M_{BH} is dissipative [12].

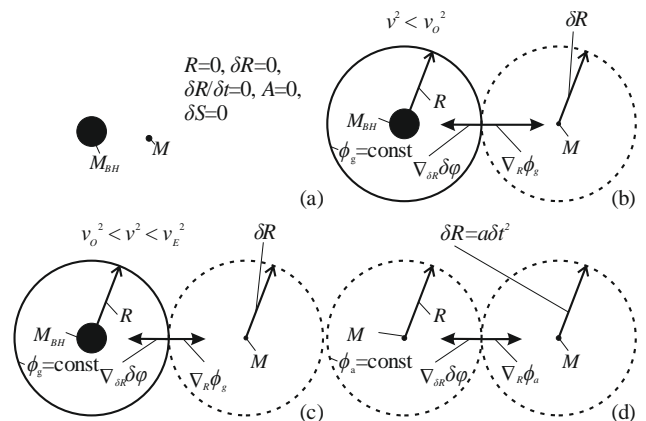


Fig. 11: Entropic work of gravity and inertia.

- (a) Free fall ($\delta R = 0$, $\delta R/\delta t = 0$, $A = 0$),
 (b) spiral trajectory fall $v < v_O$, (c) stable orbit $v_O < v < v_E$, and
 (d) inertial acceleration (not to scale).

Gradient sphere (left); entropy variation sphere (right).

As shown in Fig. 11(d), M accelerates with an acceleration of $a = \delta R/\delta t^2$ in the absence of background mass. The gradient of the inertial potential (83) provides a conceptual radius R , which defines an emergent instantaneous holographic sphere A , whereas δR provides the entropy variation sphere (50). Eventually, the conceptual R is eliminated in (81), thereby leaving only the conceptual 2^{nd} M . The gradient of the inertial potential (83) on A is normal to both sides of A as the area of the holographic

sphere A increases, as the inertial acceleration a increases and decreases as the gravitational acceleration g decreases. Furthermore, we observed that the acceleration a of M produces the conceptual R along with the corresponding variations $\delta\phi_k$ of N_A bits on a holographic sphere A . Each distribution of these bits varies from the BH equilibrium (56). Thus, in this case, $N_1(t) < N_A(t)/2$ and the mass M alone is a dissipative structure. The dissipativity of this mass, e.g. a rocket, accelerating by itself, can be attributed to the fact that the inertial acceleration can be a result of only two factors: either the rocket accelerates due to gravity or it is accelerated by an engine. In the former case, the gravity of a stellar object can pull the rocket toward its surface (Fig. 11(b)), and the rocket can either escape away or orbit around it (Fig. 11(c), dissipative case). In the latter case (Fig. 11(d)), the dissipativity is provided only by the engine of the rocket. We neglected the situation of the law of conservation of momentum (interaction of rocket with another moving object).

Therefore, the cases depicted in Fig. 11(b–d) are identical in nature. The left sphere displayed in Fig. 11 is a gradient sphere, that defines the inertial or gravitational potential along with the information capacity N_A , whereas the right sphere denotes the entropy variation sphere defining δR and N_1 . R is an artificial spatial coordinate that enables the introduction of the notion of temperature generating the potentials (25) and (80). Similar to the Bénard–Rayleigh convection, the entropic work must involve a heat transfer (38) and (39). Although the equations of motion in the abstract Newtonian dynamics are mathematically reversible in case the Planck time multiplier t is replaced by $-t$, it is not an observed behavior of the macroscopic objects modelled by these equations. Therefore, although both gravity and inertia appear to be reversible, their origin is entropic.

Any geometric considerations pertaining to the structure of \mathbb{R}^3 outside the holographic screen are unnecessary. The ancient Greek notion of geometry brings forth an unnecessary burden and axiomatization: *geo-* suggests unobservable extra-instantaneous existence, whereas *-metric* indicates the identity of indiscernibles, which is an ontological principle and the first axiom of the metric. This principle is invalid owing to the Ugly duckling theorem [36, 37] that asserts that any two distinct objects are equally similar. Additionally, the first axiom of the metric is also invalid in the quantum domain [38].

Geometric considerations are even more unnecessary if one explores the graph of nature with certain intrinsic properties that reflect the 2nd law of thermodynamics, wherein the perceived dimensionality of this graph is induced [3] by the peculiar property of the Euclidean space \mathbb{R}^4 , known as exotic \mathbb{R}^4 . Particularly, the equipotential/holographic spheres or event horizons are defined by the sets of vertices in the graph of nature with the same potential (during instantaneous observation), which attains minimum for a BH (27). Based on a geometric perspective, an event horizon is a limiting or fundamental screen with only one spherical geometric, exterior side. We used the term “holographic sphere” instead of the term “equipotential sphere”, considering the latter — which suggests permanent equality of potential — contradicts the notion of a binary message.

The anomaly observed in the cosmic microwave background radiation aligned with the plane of the Solar System and dubbed as the “Axis of Evil” [sic], implies that our intuitive concept of the physical space is incorrect. The ultimate explanation of this effect within the framework of the variational (50), binary (54), and inertial (80) potentials, which include velocity (91) and acceleration (96) relations, require further research. This effect may be due to the fact that Ampère’s right-hand grip rule induces some temperature gradient, which is substantially perpendicular to the ecliptic of the Solar System, and skewness owing to direction of the Sun’s motion.

10. Black Holes Quantum Statistics

Planck’s law for blackbody spectral radiance expressed in terms of wavelength λ is

$$B_\lambda(\lambda, T) = \frac{2hc^2}{\lambda^5} \frac{1}{\exp(hc/\lambda k_B T) - 1}. \quad (129)$$

For a BH, upon substituting $\lambda := l\ell_p$ and BH temperature (38), the above equation can be expressed as

$$B_\lambda(l, d) = \frac{2hc^2}{l^5 \ell_p^5} \frac{1}{\exp(4\pi^2 d/l) - 1}, \quad (130)$$

for wavelength or

$$B_\nu(l, d) = \frac{2hc}{l^3 \ell_p^3} \frac{1}{\exp(4\pi^2 d/l) - 1}, \quad (131)$$

for frequency (cf. Appendix 13).

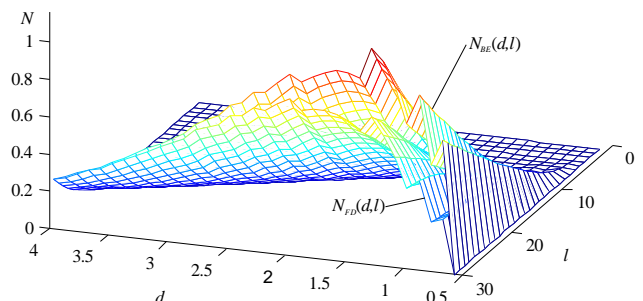


Fig. 12: Bose-Einstein (BE, top) and Fermi-Dirac (FD, bottom) 2-sphere BH statistics.

If a BH Planck area emits (absorbs) a photon (boson), as it alters its state from active ($-c^2$) to inactive (0) (or vice versa), and an electron (fermion) energy level is decreased (increased) in this interaction, the event horizon can be described using Bose–Einstein (BE) and Fermi–Dirac (FD) statistics with the degeneracy interpreted as the number of Planck areas $[zd^2]$ on the event horizon. No Planck area is distinct and each one is equally capable of emitting/absorbing energy corresponding to the wavelength multiplier l . There are certainly no dedicated microwave or X-ray areas on the horizon. Thus, these statistics along with the Maxwell–Boltzmann⁷ (MB) statistics can be described as

⁷ MB statistics lies between BE and FD statistics.

$$N_{BE}(d, l) = \frac{\lfloor \pi d^2 \rfloor}{e^{4\pi^2 d/l} - 1}, \quad (132)$$

$$N_{MB}(d, l) = \frac{\lfloor \pi d^2 \rfloor}{e^{4\pi^2 d/l}}, \quad (133)$$

$$N_{FD}(d, l) = \frac{\lfloor \pi d^2 \rfloor}{e^{4\pi^2 d/l} + 1}, \quad (134)$$

as shown in Fig. 12, where $N(d, l)$ represents the average number of bosons, classical *particles*, and fermions, respectively, with wavelength l .

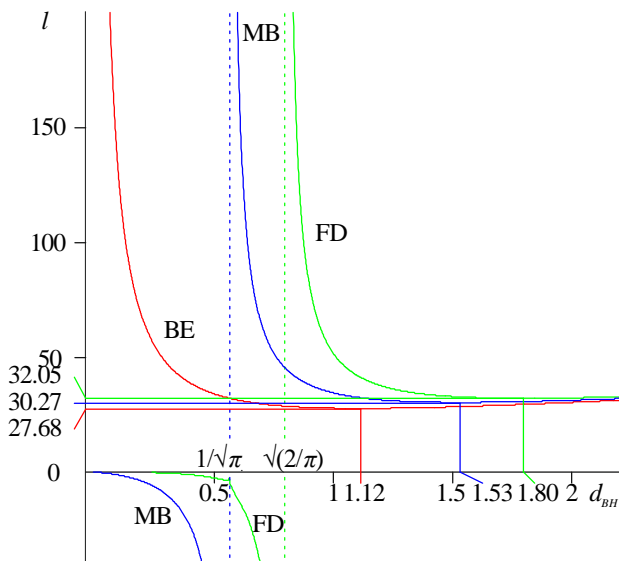


Fig. 13: Wavelength thresholds for BE (red), MB (blue), and FD (green) statistics for the 2-sphere BH as a function of its diameter multiplier d_{BH} with $N = 1$.

To emit/absorb $N > 0$ photons or correspondingly increase/decrease $N > 0$ electron energy levels on average, $N(d, l) \geq N$ and the following thresholds shown in Fig. 13 for $N = 1$ were obtained⁸ from these statistics, expressed in Eqs. (132)–(134).

$$l_{BE}(d, N) \geq \frac{4\pi^2 d}{\ln(\pi d^2 + N) - \ln(N)}, \quad (135)$$

$$l_{MB}(d, N) \geq \frac{4\pi^2 d}{\ln(\pi d^2) - \ln(N)}, \quad (136)$$

$$l_{FD}(d, N) \geq \frac{4\pi^2 d}{\ln(\pi d^2 - N) - \ln(N)}. \quad (137)$$

Each threshold poses singularity, given as

$$d_{BE}^{\text{sin}} = 0, \quad d_{MB}^{\text{sin}} = \sqrt{\frac{N}{\pi}}, \quad d_{FD}^{\text{sin}} = \sqrt{\frac{2N}{\pi}}, \quad (138)$$

and the minimum, given as

$$d_{BE}^{\text{min}} = \sqrt{-N \left(\frac{W_0(-2e^{-2}) + 2}{\pi W_0(-2e^{-2})} \right)}, \quad (139)$$

$$d_{MB}^{\text{min}} = e\sqrt{\frac{N}{\pi}}, \quad d_{FD}^{\text{min}} = \sqrt{N \frac{W_0(2e^{-2}) + 2}{\pi W_0(2e^{-2})}}$$

where $W_0(x)$ is the Lambert W function (omega function). Table 6 summarizes the minima along with the corresponding minimum wavelengths.

Perhaps, the negative wavelengths for positive diameters can be interpreted in terms of emission/absorption, wherein the positive and negative wavelengths represent the BH absorption and emission, respectively. Consequently, the BE threshold (135) with no negative wavelengths illustrates that bosons (photons) cannot escape from a BH. However, a relation between a bit (the Planck area) of a binary message (58) and a wavelength multiplier l remains to be researched.

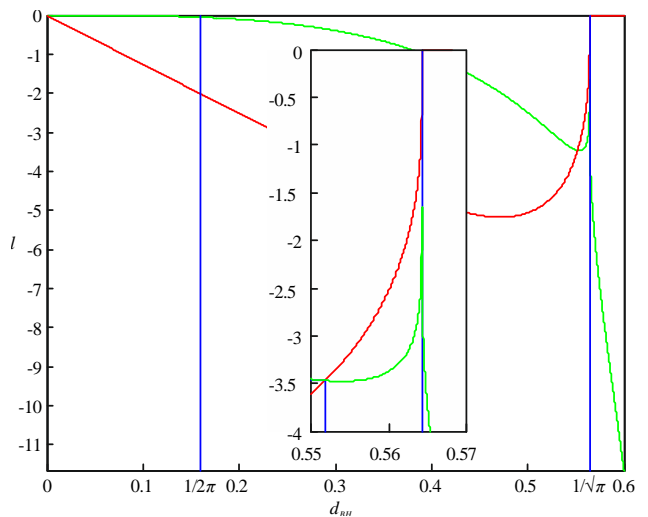


Fig. 14: Real (green) and imaginary (red) component of wavelength threshold for FD statistics as a function of d_{BH} in vicinity of $1/\sqrt{\pi}$ with $N = 1$.

Table 6: BE, MB, and FD thresholds for $N = 1, 2, \dots, 6$.

N	d_{BE}^{min}	l_{BE}^{min}	d_{MB}^{min}	l_{MB}^{min}	d_{FD}^{min}	l_{FD}^{min}
1	1.1173	27.678	1.5336	30.273	1.8007	32.054
2	1.5800	39.142	2.1689	42.812	2.5465	45.332
3	1.9352	47.939	2.6563	52.434	3.1188	55.520
4	2.2345	55.355	3.0673	60.545	3.6013	64.109
5	2.4982	61.889	3.4293	67.692	4.0264	71.676
6	2.7367	67.796	3.7566	74.152	4.4107	78.517

For $0 < d \leq \sqrt{N/\pi}$, the wavelengths l obtained from FD bound (137) are complex, as shown in Fig. 14. Below this threshold, corresponding to the diameter of a 1-bit BH for $N = 1$, BH emits complex wavelengths. After exceeding this diameter, they become *real*, and hence, observable. Presumably, only the negative and real wavelengths in the FD threshold (137) within the range $\sqrt{N/\pi} < d_{BH} \leq \sqrt{2N/\pi}$ represent the Hawking radiation of fermions. Interestingly, the real component of the wavelength below $d_{BH} = 1/(2\pi)$ Planck temperature threshold vanishes.

As described above, more detailed description of a BH interaction with the environment certainly requires further research, while considering the imaginary set of Planck

⁸ $n \leq \lfloor x \rfloor \leftrightarrow n \leq x$ (property of floor function).

units [39]. The degenerated, patternless BE BH blackbody radiation is characterized by zero Gibbs free energy, whereas the departure from degeneracy is responsible for unique spectral characteristics of stars [40].

11. Black Hole Information Paradox Solution

To illustrate the black hole information paradox that also applies to neutron stars and white dwarfs emitting patternless blackbody radiation (129), we consider two quantum, two-state *particles* (qubits) A and B entangled in one out of four maximally entangled Bell states

$$|\Phi^\pm\rangle = \frac{1}{\sqrt{2}}(|0\rangle_A |0\rangle_B \pm |1\rangle_A |1\rangle_B), \quad (140)$$

or

$$|\Psi^\pm\rangle = \frac{1}{\sqrt{2}}(|0\rangle_A |1\rangle_B \pm |1\rangle_A |0\rangle_B), \quad (141)$$

the coherence of which is maintained. If we throw one of these *particles* (say B) into a BH event horizon, we lose all the information contained in *particle B*, as asserted by the no-hiding theorem [1]. However, this information is entangled with the information support of the *particle A* through surjective isometry of the state (140) or (141). Does that mean that qubit A can no longer be measured? Or, if it can be measured, yielding - say - $|0\rangle_A$ in a basis $\{|0\rangle, |1\rangle\}$, does that mean that the *particle B* has been earlier *measured* by the BH event horizon also as $|0\rangle_B$ (in the case of $|\Phi^\pm\rangle$) or $|1\rangle_B$ (in the case of $|\Psi^\pm\rangle$)?

Certainly not. Even if a BH horizon is a quantum system, it cannot stand in the role of an observer [41, 42]. Patternless BH horizon contradicts the entanglement between A and B defined by Eqs. (140) or (141). Any state of the orthonormal basis of four Bell states in a Hilbert space \mathbb{C}^4 is a unique pattern among uncountably infinite number of other possible quantum states. Therefore, BH would destroy coherence of the entangled state transforming it into a separable state

$$|\varphi\rangle = \frac{1}{2}(|0\rangle_A |0\rangle_B \pm |0\rangle_A |1\rangle_B \pm |1\rangle_A |0\rangle_B \pm |1\rangle_A |1\rangle_B), \quad (142)$$

from which the measurement of A will yield an arbitrary, equally probable result. Principle of locality is invalid in the quantum domain [43]. Considering a BH horizon as a quantum system, the Margolus–Levitin theorem and Eq. (64) set a bound on a minimum time period required for the BH to transfer from one state to another, orthogonal one, given (with (64)) as

$$\delta t_{ML} \geq \frac{\pi \hbar}{2E_{BH}} = \frac{2\pi}{d_{BH}} t_P, \quad (143)$$

and constraining to $\delta t_{ML} \geq t_P$, gives $d_{BH} \leq 2\pi$, as a maximum BH diameter, allowing for such a transformation. The meaning of orthogonality of a BH binary message requires further research. Much of the essence of quantum theory already makes itself known in the case of just two nonorthogonal states [30].

These limits do not hold for an observation of *particle B* on a holographic sphere, as shown in Fig. 8. If B is a photon, observed visually through an eye of a living or-

ganism, its photoisomerization induced signal transduction cascade will provide a definite result preserving entanglement. In other words, the information obtained from the measured qubit B will penetrate to the interior of the observer through a Planck area ℓ_P^2 on a holographic sphere, as one bit of classical information. This cannot happen for an interior-less BH shown in Fig. 2(b).

12. Discussion

This study aimed to define BHs (13) as interior-less entities emitting degenerate, patternless binary messages (56), whereas $D_{BH} = \ell_P/(2\pi)$ represented Big Bang singularity. Micro-BHs are inherently unstable and prone to collapses [20], and hence, this study delivered further arguments in support of this claim. BH threshold of distinguishability (10) was found to be a threshold of BH collapsibility (22). Temperature uncertainty for one degree of freedom is equal to the Planck temperature if time uncertainty equals Planck time (67), whereas π degrees of freedom enable the recovery (68) of exact Unruh (38) and Hawking (39) temperature equations. The variational potential (50) can be expressed as the ratio of the number of the active Planck areas to the information capacity of the holographic sphere, whereas the entropic work is the product of the test mass and the variational potential (81).

A relation between a bit of a binary message (58) and wavelength multiplier l of a blackbody radiation requires further research, and may shed a new light on the observed “Axis of Evil” anomaly. An in-depth study of BH interaction with the environment is required.

Perhaps the most striking conclusion of this study is that every dissipative structure is a sphere in nonequilibrium thermodynamic condition, provided with an interior. Interiors of living cells were exploited by biological evolution, probably beginning with coacervates. An open question is why would a hurricane need an interior?

Acknowledgements

I truly thank my wife for her support. I would like to thank Mirek for the insightful discussions and encouragement, especially for noting that a bit is inadequate to be meaningfully assigned to the notion of the potential and that BHs invalidate the Jordan–Brouwer separation theorem, in addition to assisting while solving the sign riddle. I would like to thank my godson Lars for meticulously spotting typographical errors and missing commas. I also thank Piotr for the helpful discussions and finding certain logical loopholes in the paper, along with noting that the effect of Axis of Evil could be due to Ampère’s right-hand grip rule.

-
- [1] Samuel L. Braunstein, Arun K. Pati, “Quantum Information Cannot Be Completely Hidden in Correlations: Implications for the Black-Hole Information Paradox”. Feb 2007. <https://doi.org/10.1103/PhysRevLett.98.080502>
 - [2] John Archibald Wheeler, “Proceedings of the 3rd International Symposium Foundations of Quantum Mechanics in the Light of New Technology” 1989. ISBN 4890270035
 - [3] Szymon Łukaszyk, “Four Cubes”. Jul 2020. [arXiv:2007.03782](https://arxiv.org/abs/2007.03782) [math.GM]
 - [4] Ludwig Boltzmann, “Über die Beziehung zwischen dem zweiten Hauptsatze des mechanischen Wärmethorie und

- der Wahrscheinlichkeitsrechnung, respective den Sätzen über das Wärmegleichgewicht". 1877.
<https://doi.org/10.1017/CBO9781139381437.011>
 available. at
<http://users.polytech.unice.fr/~leroux/boltztrad.pdf>.
- [5] Thomas S. Kuhn, "Black-Body Theory and the Quantum Discontinuity, 1894-1912". 1978.
<https://doi.org/10.1021/ed057pA242.3>
- [6] Maximilian Schlosshauer, et al., "A Snapshot of Foundational Attitudes Toward Quantum Mechanics". Jan 2013.
<https://doi.org/10.1016/j.shpsb.2013.04.004>
- [7] Pierre Teilhard de Chardin, "The Phenomenon of Man". 1955.
 ISBN 978-0-06-163265-5
- [8] Rudolf Carnap, "The philosophy of Rudolf Carnap". 1963.
 ISBN 978-0812691535.
- [9] Časlav Brukner, "A No-Go Theorem for Observer-Independent Facts". Apr 2018.
<https://doi.org/10.3390/e20050350>
- [10] Massimiliano Proietti, et al, "Experimental Rejection of Observer Independence in the Quantum World". Sep 2019.
<https://doi.org/10.1126/sciadv.aaw9832>
- [11] Kok-Wei Bong, et al., "Testing the Reality of Wigner's Friend's Experience". Dec 2019.
<https://doi.org/10.1117/12.2540002>
- [12] Ilya Prigogine, Isabelle Stengers, "Order out of Chaos: Man's New Dialogue with Nature". Apr 1984.
 ISBN 434-603953
- [13] Gerard 't Hooft, "Dimensional Reduction in Quantum Gravity". Oct 1993.
[arXiv:gr-qc/9310026](https://arxiv.org/abs/gr-qc/9310026).
- [14] Sabine Hossenfelder, "Comments on and Comments on Comments on Verlinde's paper "On the Origin of Gravity and the Laws of Newton". Mar 2010.
[arXiv:1003.1015v1 \[gr-qc\]](https://arxiv.org/abs/1003.1015v1).
- [15] Max Planck, "Über Irreversible Strahlungsvorgänge". 1899.
- [16] Anil N. Hirani, "Discrete Exterior Calculus". 8 Jun 2003.
<https://doi.org/10.7907/ZHY8-V329>
- [17] Mathieu Desbrun, et al., "Discrete Differential Forms for Computational Modeling". 2008.
https://doi.org/10.1007/978-3-7643-8621-4_16
- [18] Jacob Bekenstein, "Black Holes and Entropy". Apr 73.
<https://doi.org/10.1103/PhysRevD.7.2333>
 (http://www.scholarpedia.org/article/Bekenstein_bound,
http://www.scholarpedia.org/article/Bekenstein-Hawking_entropy).
- [19] Leonard Susskind, "Black Hole War: My Battle with Stephen Hawking to Make the World Safe for Quantum Mechanics". Jul 2008.
 ISBN 978-0316016407
- [20] Stephen Hawking, "Black Hole Explosions?". Mar 1974.
<https://doi.org/10.1038/248030a0>
 (http://www.scholarpedia.org/article/Hawking_radiation)
- [21] Szymon Łukaszyk, "A Simple Recursive Formula for Volumes and Surfaces of n -balls". May 2020
<https://doi.org/10.13140/RG.2.2.14751.38566>
- [22] G. Parisi, N. Sourlas, "Random Magnetic Fields, Supersymmetry, and Negative Dimensions". Sep 1979.
<https://doi.org/10.1103/PhysRevLett.43.744>
- [23] Erik Verlinde, "On the Origin of Gravity and the Laws of Newton". Jan 2010.
[https://doi.org/10.1007/JHEP04\(2011\)029](https://doi.org/10.1007/JHEP04(2011)029)
- [24] Margot M. Brouwer, et al., "First test of Verlinde's theory of Emergent Gravity using Weak Gravitational Lensing measurements". 9 Dec 2016.
<https://doi.org/10.1093/mnras/stw3192>
- [25] Arieh Ben-Naim, "Farewell to Entropy, Statistical Thermodynamics Based on Information". Jan 2008.
<https://doi.org/10.1142/6469>
- [26] Espen Gaarder Haug, "Finding the Planck Length Multiplied by the Speed of Light Without any Knowledge of G , c , or \hbar , using a Newton force spring". Jul 2020.
<https://doi.org/10.1088/2399-6528/ab9dd7>
- [27] Gregory J. Chaitin, "On the Length of Programs for Computing Finite Binary Sequences". Oct. 1966.
<https://doi.org/10.1145/321356.321363>
- [28] R. Landauer, "Irreversibility and Heat Generation in the Computing Process". Jul 1961.
<https://doi.org/10.1147/rd.53.0183>
- [29] Aharon Davidson, "From Planck Area to Graph Theory: Topologically Distinct Black Hole Microstates". Oct 2019.
<https://doi.org/10.1103/PhysRevD.100.081502>
- [30] Christopher A. Fuchs, "Just two nonorthogonal quantum states". 12 Oct 1998.
https://doi.org/10.1007/0-306-47097-7_2
- [31] Fabio Scardigli, "Some Heuristic Semiclassical Derivations of the Planck Length, the Hawking Effect and the Unruh Effect". Feb 1995.
<https://doi.org/10.1007/BF02726152>
- [32] Blaise Goutéraux, "Black-Hole Solutions to Einstein's Equations in the Presence of Matter and Modifications of Gravitation in Extra Dimensions". Nov 2010.
[arXiv:1011.4941 \[hep-th\]](https://arxiv.org/abs/1011.4941)
- [33] Galina Weinstein, "Einstein's Uniformly Rotating Disk and the Hole Argument". Apr 2015.
[arXiv:1504.03989 \[physics.hist-ph\]](https://arxiv.org/abs/1504.03989)
- [34] Steven Weinberg, "Gravitation and Cosmology". 1972.
 ISBN 978-0-471-92567-5
- [35] Pentti Kanerva, "Sparse Distributed Memory". 1988.
 ISBN 978-0-262-11132-4
- [36] Satoshi Watanabe, "Knowing and Guessing: A Quantitative Study of Inference and Information". 1969.
 ISBN 0-471-92130-0. LCCN 68-56165
- [37] Satoshi Watanabe, "Epistemological Relativity - Logico-Linguistic Source of Relativity". Mar 1986.
<https://doi.org/10.4288/jafpos1956.7.1>
- [38] Szymon Łukaszyk, "New Concept of Probability Metric and its Applications in Approximation of Scattered Data Sets". Mar 2004.
<https://doi.org/10.1007/s00466-003-0532-2>
- [39] Szymon Łukaszyk, "A Short Note About Graphene and the Fine Structure Constant". Oct 2020.
<https://doi.org/10.13140/RG.2.2.21718.88641>
- [40] D. S. Kothari, B. N. Singh, "Bose-Einstein Statistics and Degeneracy". Jun 1941.
<https://doi.org/10.1098/rspa.1941.0049>
- [41] Časlav Brukner, "Qubits are not Observers – a No-Go Theorem". Jul 2021.
[arXiv:2107.03513 \[quant-ph\]](https://arxiv.org/abs/2107.03513)
- [42] Jacques Pienaar, "A quintet of Quandaries: Five No-Go Theorems for Relational Quantum Mechanics". Sep 2021.
<https://doi.org/10.1007/s10701-021-00500-6>.
- [43] John Stewart Bell, "On the Einstein Podolsky Rosen Paradox". Nov 1964.
<https://doi.org/10.1103/PhysicsPhysiqueFizika.1.195>
- [44] Sheldon Axler, et al., "Harmonic Function Theory". 4 May 2006.
 ISBN 978-1-4899-1186-5
- [45] Tsogtgerel Gantumur, "[Harmonic functions](#)". McGill University, Math 314.

Appendices

1. The alternative form of BH (Hawking) temperature (38) is given as

$$\begin{aligned} T &= \frac{T_P}{2\pi d} = \frac{T_P}{2\pi} \frac{\ell_P}{2R_{BH}} = \frac{T_P \ell_P}{4\pi} \frac{c^2}{2GM_{BH}} = \\ &= \frac{c^2}{8\pi GM} \sqrt{\frac{\hbar c^5}{Gk_B^2}} \sqrt{\frac{\hbar G}{c^3}} = \frac{\hbar c^3}{8\pi Gk_B M_{BH}} \end{aligned} \quad (144)$$

2. The alternative form of Planck–Einstein (Compton) relation is given as

$$\begin{aligned} E = h\nu &= h \frac{c}{\lambda} = \frac{hc}{l\ell_P} = \frac{2\pi\hbar c}{l} \sqrt{\frac{c^3}{\hbar G}} = \\ &= \frac{2\pi}{l} \frac{k_B}{k_B} \sqrt{\frac{\hbar^2 c^2 c^3}{\hbar G}} = \frac{2\pi}{l} k_B T_P \end{aligned} \quad (145)$$

3. BH diameter fluctuations

After the absorption/emission of a wavelength l , the 2-sphere BH diameter defined by its mass increases(+)/decreases(−) owing to the Compton mass $M = h/(c\lambda)$ of this wavelength. Therefore,

$$\begin{aligned} D_{BH}^{A/E} &= D_{BH} \pm \delta D = d\ell_P \pm \frac{4G}{c^2} \frac{2\pi\hbar}{c l \ell_P} \\ &= d\ell_P \pm \frac{8\pi\hbar G}{lc^3 \ell_P} = d\ell_P \pm \frac{8\pi\ell_P}{l} = (d \pm 8\pi/l) \ell_P \end{aligned} \quad (146)$$

Accordingly, the BH area increases/decreases, such that

$$\begin{aligned} A_{BH}^{A/E} &= \pi \left(d^{A/E} \right)^2 \ell_P^2 = \pi \left(d\ell_P \pm \frac{8\pi\hbar G}{c^3 l \ell_P} \right)^2 \\ \pi \left(d^{A/E} \right)^2 \ell_P^2 &= \pi \left(d\ell_P \pm \frac{8\pi}{l} \ell_P \right)^2 = \\ &= \pi \ell_P^2 \left(d \pm \frac{8\pi}{l} \right)^2 \end{aligned} \quad (147)$$

If $l = d/2$ [18, 19] then

$$d_{k+1}^{A/E} = \pm \sqrt{256\pi^2 \frac{1}{d_k^2} \pm 32\pi + d_k^2} \quad (148)$$

4. BH diameter (20) after absorption or emission of a wavelength l in dimensions $n = 2, 3, \dots, 5$.

n	$(d_{k+1}^{A/E})^{n-1}$
2	$d_k \pm 8\pi l$
3	$d_k^2 \pm 16\pi d_k/l + 64\pi^2/l^2$
4	$d_k^3 \pm 24\pi d_k^2/l + 192\pi^2 d_k/l^2 \pm 512\pi^3/l^3$
5	$d_k^4 \pm 32\pi d_k^3/l + 384\pi^2 d_k^2/l^2 \pm 2048\pi^3 d_k/l^3 + 4096\pi^4/l^4$

5. Negative and imaginary unit lengths.

There are four possibilities for the volume of unit n -cubic element a^n in n -dimensional space in dependence on what we take as the unit length $a = \{1, -1, i, -i\}$:

$$a = 1 \quad a^n = 1 \quad n \in \mathbb{C}, \quad (149)$$

$$a = -1 \quad a^n = \begin{cases} 1 & n \text{ is even} \\ -1 & n \text{ is odd} \\ \mathbb{C} & n \in \mathbb{R} \setminus \mathbb{Z} \cup n \in \mathbb{C} \end{cases}, \quad (150)$$

$$a = i \quad a^n = \begin{cases} 1 & n = \pm 0, 4, 8, \dots \\ -1 & n = \pm 2, 6, 10, \dots \\ i & n = \dots, -7, -3, 1, 5, 9, \dots \\ -i & n = \dots, -9, -5, -1, 3, 7, \dots \\ \mathbb{C} & n \in \mathbb{R} \setminus \mathbb{Z} \cup n \in \mathbb{C} \end{cases}, \quad (151)$$

$$a = -i \quad a^n = \begin{cases} 1 & n = \pm 0, 4, 8, \dots \\ -1 & n = \pm 2, 6, 10, \dots \\ i & n = \dots, -9, -5, -1, 3, 7, \dots \\ -i & n = \dots, -7, -3, 1, 5, 9, \dots \\ \mathbb{C} & n \in \mathbb{R} \setminus \mathbb{Z} \cup n \in \mathbb{C} \end{cases} \quad (152)$$

The unit length a is a scaling factor of a relationship between the vertices of the graph of nature. Generally, it can be real (positive or negative) or imaginary (positive or negative), and this list may not be exhaustive. Any vertex beyond the countably infinite number of vertices can exhibit any relationship with other vertices. However, only a real and positive unit length (149) yields a real and positive unit n -cubic element a^n for any complex dimension n .

6. Bekenstein-Hawking entropy (44) from Verlinde Eq. (46)

$$\begin{aligned} \delta S &= 2\pi k_B \frac{Mc}{\hbar} \delta R = -2\pi k_B \frac{M_{BH} c}{\hbar} R_{BH} = \\ &= -2\pi k_B \frac{c}{\hbar} \frac{R_{BH} c^2}{2G} R_{BH} = -\frac{\pi k_B R_{BH}^2}{\ell_P^2} = \\ &= -\frac{1}{4} k_B N_{BH} \end{aligned} \quad (153)$$

where Eq. (87) was substituted and the sign was reversed.

7. BH temperature vs. BH energy/work

Comparing dimensionless BH temperature with dimensionless BH energy yields

$$\frac{T_{BH}}{T_P} = \frac{1}{2\pi d_{BH}}, \quad \frac{E_{BH}}{E_P} = \frac{d_{BH}}{4} \Rightarrow d_{BH} = \pm \sqrt{\frac{2}{\pi}}, \quad (154)$$

that is d_{BH} of a minimum 2-bit BH and the 1st singularity (138) of the FD statistics.

Comparing dimensionless BH temperature with BH entropic work (63) yields

$$\frac{T_{BH}}{T_P} = \frac{1}{2\pi d_{BH}}, \frac{W_{BH}}{E_P} = \frac{d_{BH}}{8} \Rightarrow d_{BH} = \pm \sqrt{\frac{4}{\pi}}, \quad (155)$$

that is d_{BH} of a minimum 4-bit BH, one unit of BH entropy (44), and the 2nd singularity (138) of the FD statistics.

Comparing BH mass–energy equivalence (64) with the Landauer limit yields

$$\begin{aligned} M_{BH} c^2 &= T_{BH} k_B \ln(2) \\ \frac{d_{BH} \ell_P c^2}{4G} c^2 &= \frac{T_P}{2\pi d_{BH}} k_B \ln(2) \\ \frac{d_{BH} c^4}{4G} \sqrt{\frac{\hbar G}{c^3}} &= \sqrt{\frac{\hbar c^5}{G k_B^2}} \frac{k_B \ln(2)}{2\pi d_{BH}} \\ \frac{d_{BH}}{2} &= \frac{\ln(2)}{\pi d_{BH}} \quad d_{BH} = \sqrt{2} \sqrt{\frac{\ln(2)}{\pi}} \approx 0.6643 \\ N_{BH} &= \pi d_{BH}^2 = 2 \ln(2) \approx 1.3863 \end{aligned} \quad (156)$$

Comparing BH entropic work (63) with the Landauer limit, or equivalently, the BH entropy with the Landauer limit entropy yields

$$\begin{aligned} \frac{1}{2} M_{BH} c^2 &= T_{BH} k_B \ln(2) \quad \text{or} \\ \frac{1}{4} k_B N_{BH} &= k_B \ln(2) \\ N_{BH} &= 4 \ln(2) = \pi d_{BH}^2 \approx 2.7725 \\ d_{BH} &= 2 \sqrt{\frac{\ln(2)}{\pi}} \approx 0.9394 \end{aligned} \quad (157)$$

8. Variational potential on a BH horizon

$$\frac{4\pi c^2}{N_{BH}} \frac{R_{BH}}{\hat{\lambda}_M} = -\frac{c^2}{2}, \quad (158)$$

$$\frac{4\pi c^2}{N_{BH}} \frac{R_{BH}}{\hat{\lambda}_M} = \frac{4\pi c^2}{4\pi R_{BH}^2 / \ell_P^2} \frac{R_{BH}}{\hat{\lambda}_M} = -\frac{c^2}{2}, \quad (159)$$

$$\hat{\lambda}_M = -\frac{2\ell_P^2}{R_{BH}} = -\hat{\lambda}_{BH}. \quad (160)$$

Furthermore,

$$N_{BH} = \frac{4\pi R_{BH}^2}{\ell_P^2} \Leftrightarrow R_{BH} = \pm \sqrt{\frac{N_{BH}}{4\pi}} \ell_P, \quad (161)$$

so

$$\hat{\lambda}_{BH} = \pm 2\ell_P \sqrt{\frac{4\pi}{N_{BH}}} \Leftrightarrow \hat{\lambda}_M = \mp 2\ell_P \sqrt{\frac{4\pi}{N_{BH}}}. \quad (162)$$

9. Planck units' derivation

Although this derivation is probably established, it has not been determined by the author. We begin with the measured speed of light c and define it to be a quotient of a length unit (ℓ_P) and a time unit (t_P): $c = \ell_P/t_P$. Thereafter, we define a unit of acceleration (a_P) as the time unit required to achieve the speed of light: $a_P = c/t_P$. Subsequently, we assumed an inertial force equal to gravitational force between two such mass units (m_P) distanced by the length unit

$$m_P a_P = G \frac{m_P m_P}{\ell_P^2}. \quad (163)$$

Ultimately, a Compton wavelength or Planck–Einstein relation (they are equivalents) for the mass unit is required, which is expressed as

$$m_P = \frac{h}{c\lambda} \Leftrightarrow m_P c^2 = h\nu = h \frac{c}{\lambda}. \quad (164)$$

Next, we consider the reduced $\hbar = h/2\pi$ and presume the wavelength to be $\lambda = 2\pi\ell_P$. The remaining derivation is posed as an exercise for the reader.

Overall, the simplest derivation of Planck units, based on HUP, mass–energy equivalence, Schwarzschild radius, and $c = \delta R/\delta t$ is presented in [31].

10. Hawking temperature from equipartition theorem

BH mass–energy equivalence can be stated as

$$E_{BH} = M_{BH} c^2. \quad (165)$$

If the BH energy is uniformly divided over N_{BH} bits on the horizon, the temperature can be determined using the equipartition rule for a single degree of freedom (one bit), which is expressed as

$$E_{BH} = \frac{1}{2} k_B N_{BH} T_{BH}, \quad (166)$$

from which relation we can recover the Hawking temperature as

$$T_{BH} = \frac{M_{BH} c^2 \ell_P^2}{2\pi k_B R_{BH}^2}. \quad (167)$$

11. Potential in negative dimensions

If a spherically symmetric fundamental solution (potential) ϕ of the Laplace's equation and the general Poisson's equation exists in \mathbb{R}^n , it must be in the form of [44, 45]

$$\phi_n = \begin{cases} \frac{R^{2-n}}{n(2-n)V_n} & \text{for } n \neq 2 \\ \frac{1}{2\pi} \log(R) & \text{for } n = 2 \end{cases}, \quad (168)$$

where $R \neq 0$ and V_n represents the surface area of the unit n -ball. This can be evaluated in the negative dimensions, as shown in Fig. 15 for $R = 1$.

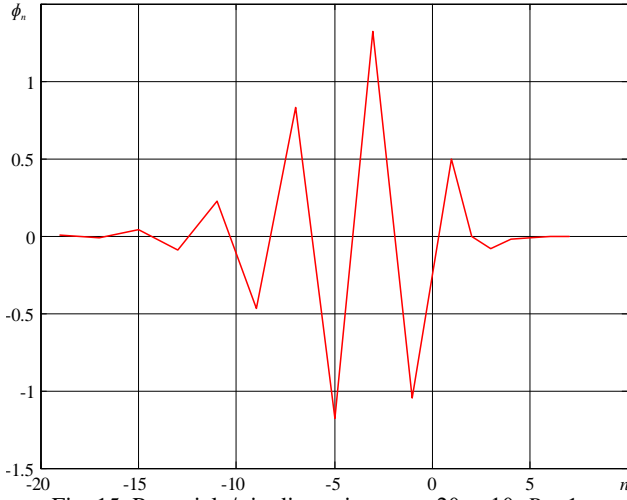


Fig. 15: Potential ϕ_n in dimensions $n = -20, \dots, 10$, $R = 1$.

Further research is required to evaluate the possible relation of the logarithmic potential (168) in \mathbb{R}^2 with Shannon information entropy (60) and Landauer bound (61), (156), or (157).

12. Lorentz contraction and velocity bound

From Eqs. (90), (104), and (105), the velocity bound (91) is derived as

$$\frac{\delta L^2}{\delta t^2} - \frac{\delta R^2}{\delta t^2} = c^2. \quad (169)$$

Furthermore, the squared-Lorentz contraction (93) can be expressed as

$$\delta L^2 = -\frac{\delta L_0^2}{c^2} \frac{\delta R^2}{\delta t^2}, \quad (170)$$

from which equation we substitute $c^2 \delta t^2$ into the first equation to reduce it to be time independent.

13. Planck law

We set

$$A_\lambda \doteq \frac{2h}{\ell_p^5} c^2, \quad A_\nu \doteq \frac{2h}{\ell_p^3} c^2, \quad (171)$$

in Planck's laws for BH spectral radiance (130), (131). Their derivatives w/r/t l are (derivatives w/r/t d are monotonic)

$$\frac{\partial B_\lambda(l, d)}{\partial l} = \frac{4A_\lambda d \pi^2 \exp(4\pi^2 d/l)}{l^7 (\exp(4\pi^2 d/l) - 1)^2} - \frac{5A_\lambda}{l^6 (\exp(4\pi^2 d/l) - 1)} \quad (172)$$

$$\frac{\partial B_\nu(l, d)}{\partial l} = \frac{4A_\nu d \pi^2 \exp(4\pi^2 d/l)}{l^5 (\exp(4\pi^2 d/l) - 1)^2} - \frac{3A_\nu}{l^4 (\exp(4\pi^2 d/l) - 1)} \quad (173)$$

From Eqs. (172) and (173), we can determine the wavelength multiplier l maximizing spectral radiance at a given BH diameter d in terms of the maximum radiation wavelength λ

$$d_\lambda^{\max} = \frac{l}{4\pi^2} (W_0(-5e^{-5}) + 5) =, \quad (174)$$

$$= 0.125767812719937l$$

$$l_\lambda^{\max} = 7.951159986d, \quad (175)$$

or of the maximum radiation frequency ν

$$d_\nu^{\max} = \frac{l}{4\pi^2} (W_0(-3e^{-3}) + 3) =, \quad (176)$$

$$= 0.071467894189626l$$

$$l_\nu^{\max} = 13.99229698d, \quad (177)$$

where $W_0(x)$ is the Lambert W function.

It can be seen that the maximum emitted wavelength of BH in the visible radiation range ($1 \mu\text{m} \rightarrow l = 6.19\text{E}28$) exhibit a diameter of $d_{BH} = 7.78\text{E}+27 \rightarrow D_{BH} = 1.26\text{E}-7$ m, whereas the maximum emitted wavelength of Sagittarius A* ($D_{BH} \approx 2.56\text{E}10$ m) amounts $\lambda = 2.04\text{E}+11$ m, which is more than 100 times larger than ELF radio waves of $1\text{E}8$ m (≈ 3 Hz).

14. Certain properties of the Shannon entropy of holographic spheres

$$H(k) = \log(k) - \frac{k-1}{k} \log(k-1). \quad (178)$$

The 1st derivative is

$$\frac{dH}{dk} = -\frac{\log(k-1)}{k^2}, \quad (179)$$

yielding the maximum of $H(k)$ at $k = 2$. The 2nd derivative

$$\frac{d^2 H}{dk^2} = \frac{2(k-1)\log(k-1) - k}{k^3(k-1)}, \quad (180)$$

yields the inflection point of $H(k)$ at

$$k = \frac{1}{2W_0\left(\frac{1}{2}e^{-\frac{1}{2}}\right)} + 1 \approx 3.0935. \quad (181)$$

The integral is

$$\int H dk = (\log(k-1) + k) \log(k) - (k-1) \log(k-1) + \text{Li}_2(1-k), \quad (182)$$

where $\text{Li}_2(z)$ denotes dilogarithm.